

# $N$ -widths, sup-infs, and optimality ratios for the $k$ -version of the isogeometric finite element method

John A. Evans, Yuri Bazilevs, Ivo Babuška, and Thomas J.R. Hughes

## Abstract

We begin the mathematical study of the  $k$ -method utilizing the theory of Kolmogorov  $n$ -widths. The  $k$ -method is a finite element technique where spline basis functions of higher-order continuity are employed. It is a fundamental feature of the new field of isogeometric analysis. In previous works, it has been shown that using the  $k$ -method has many advantages over the classical finite element method in application areas such as structural dynamics, wave propagation, and turbulence.

The Kolmogorov  $n$ -width and sup-inf were introduced as tools to assess the effectiveness of approximating functions. In this paper, we investigate the approximation properties of the  $k$ -method with these tools. Following a review of theoretical results, we conduct a numerical study in which we compute the  $n$ -width and sup-inf for a number of one-dimensional cases. This study sheds further light on the approximation properties of the  $k$ -method. We finish this paper with a comparison study of the  $k$ -method and the classical finite element method and an analysis of the robustness of polynomial approximation.

## 1 Introduction

In this paper we present a theoretical and computational framework that allows one to examine approximation properties of a prescribed discretization. The framework presented in this paper is based on the theory of Kolmogorov  $n$ -widths. This theory defines and gives a characterization of optimal  $n$ -dimensional spaces for approximating function classes and their associated errors.  $N$ -widths are a well-explored subject in approximation theory, but they are not as familiar to the finite element and computational mechanics communities.

A practically useful concept that emerges from the theory of  $n$ -widths is the sup-inf. Sup-infs quantify the error induced by a particular discretization in approximating a given class of functions. In the context of Hilbert spaces, sup-infs can be directly computed by way of the solution of a variational eigenproblem. As error is exactly quantified, sup-infs can distinguish between two methods of the same approximation order. Although such distinctions are rarely made in classical approximation theory of finite elements, we feel that such comparisons are necessary, primarily due to the advent of new computational technologies. For example,  $C^0$ - and  $C^1$ -continuous quadratic finite elements deliver the same asymptotic convergence rate, but the size of the approximation errors for the two classes of functions will be different.

By comparing the sup-inf to the  $n$ -width, we are able to assess the performance of a given approximation space with respect to the optimal discretization.

Recently Babuska *et al.* [4] made use of  $n$ -widths and sup-infs to assess approximation properties of functions employed in generalized finite element methods. In this paper, we apply this framework to the study of one-dimensional spline spaces of variable order and continuity. Particular instantiations of these spaces include classical  $C^0$ -continuous finite elements as well as global polynomials. The emphasis of our study is spline functions of maximal continuity. Such functions are the basis of the  $k$ -version of the isogeometric finite element method. The concept of isogeometric analysis was first introduced in [21]. The developments of [21] aimed at unifying geometrical modeling and analysis for engineering applications. Although the development of isogeometric analysis was driven by the need of a tighter link between computer-aided design and computer-aided analysis, using spline functions in analysis has proven to be beneficial from the standpoint of solution accuracy. Recent results in structural vibrations [15, 16], wave propagation [22], and turbulent flow [1, 8] indicate that on a per-degree-of-freedom basis, discretizations of higher continuity are superior to their  $C^0$ -continuous counterparts.

In Section 2, we give an overview of spline functions, their construction, and their properties and define four discrete function spaces used for the analysis in this paper. In Section 3, we outline particular function classes of interest that arise in the study of partial differential equations that we wish to approximate with spline functions. These classes of interest include standard Sobolev spaces, Sobolev spaces with periodic boundary conditions, and Jacobi-weighted Sobolev spaces. In Section 4, we introduce terminology and concepts and state classical results of the theory of  $n$ -widths and sup-infs. In this section, we also present known theoretical results on the optimality of splines for function classes of interest. In Section 5, we outline a computational framework for the evaluation of  $n$ -widths and sup-infs and apply this framework to a number of one-dimensional cases. In Section 6, we draw conclusions based on our studies.

## 2 Splines

This section gives a very brief overview of univariate B-splines and periodic splines. B-splines were first introduced by Schoenberg in 1946 [28] in the attempt of developing piecewise polynomials with prescribed smoothness properties. In his 1972 paper, de Boor [11] introduced a simple and stable recursion formula for evaluating them, and since then, B-splines have been a standard in the numerical analysis and computer-aided geometric design communities. For an overview of splines, their properties, and robust algorithms for evaluating their values and derivatives, see de Boor [12] and Schumaker [29]. For an introductory text on non-uniform rational B-splines (NURBS), see Rogers [27], while more detailed treatments are given in the books of Piegl and Tiller [25] and Cohen, Riesenfeld, and Elber [14]. For the application of splines to finite element analysis, see Höllig [20] and Hughes, Cottrell, and Bazilevs [21].

A *B-spline* basis is comprised of piecewise polynomials joined with prescribed continuity. In order to define a B-spline basis of polynomial order  $p$  in one dimension one needs the notion of a *knot vector*. A knot vector in one dimension is a set of coordinates in the parametric space, written as  $\Xi = \{\xi_1, \xi_2, \dots, \xi_{n+p+1}\}$ , where  $i$  is the knot index,  $i = 1, 2, \dots, n + p + 1$ ,

$\xi_i \in \mathbb{R}$  is a knot,  $\xi_1 \leq \xi_2 \leq \dots \leq \xi_{n+p+1}$ , and  $n$  is the total number of basis functions.

Given  $\Xi$  and  $p$ , B-spline basis functions are constructed recursively starting with piecewise constants ( $p = 0$ ):

$$B_{i,0}(\xi) = \begin{cases} 1 & \text{if } \xi_i \leq \xi < \xi_{i+1} \\ 0 & \text{otherwise.} \end{cases} \quad (1)$$

For  $p = 1, 2, 3, \dots$ , they are defined by

$$B_{i,p}(\xi) = \frac{\xi - \xi_i}{\xi_{i+p} - \xi_i} B_{i,p-1}(\xi) + \frac{\xi_{i+p+1} - \xi}{\xi_{i+p+1} - \xi_{i+1}} B_{i+1,p-1}(\xi). \quad (2)$$

When  $\xi_{i+p} - \xi_i = 0$ ,  $\frac{\xi - \xi_i}{\xi_{i+p} - \xi_i}$  is taken to be zero, and similarly, when  $\xi_{i+p+1} - \xi_{i+1} = 0$ ,  $\frac{\xi_{i+p+1} - \xi}{\xi_{i+p+1} - \xi_{i+1}}$  is taken to be zero.

We define

$$S(n, p, \Xi) = \text{span} \{B_{1,p}(\xi), B_{2,p}(\xi), \dots, B_{n,p}\} \quad (3)$$

to be a B-spline space of dimension  $n$  with degree  $p$  and built using knot vector  $\Xi$ . B-spline basis functions form a partition of unity, each one is compactly supported on the interval  $[\xi_i, \xi_{i+p+1}]$ , and they are point-wise non-negative. These properties are important and make these functions attractive for use in analysis.

The first and last knots are called *end knots*, and the other knots are called *interior knots*. Note that knots may be repeated. A knot vector is said to be *open* if its end knots have multiplicity  $p + 1$ . Basis functions formed from an open knot vector are interpolatory at end knots of the parametric interval but they are not, in general, interpolatory at interior knots. Basis functions of order  $p$  have  $p - 1$  continuous derivatives at non-repeated knots. If a knot has multiplicity  $k$ , then the number of continuous derivatives decreases by  $k - 1$ . When the multiplicity of a knot is exactly  $p$ , the basis function is interpolatory and only  $C^0$ -continuous at that knot.

*Periodic splines* are constructed from B-splines subject to periodic boundary conditions. If one desires a periodic spline space that is  $C^{s-1}$  at the end knots, one must directly enforce this constraint onto the associated B-spline space by restricting the first  $s - 1$  derivatives at the end knots to be equal.

The above constructions (1)-(2) encompass a large class of functions. All the finite dimensional spaces considered in this paper may be expressed using particular instantiations of the knot vector  $\Xi$ . In particular, we define the following discrete spline spaces:

- $K(n, k, a, b)$  is the B-spline space of dimension  $n$  and degree  $k$  corresponding to an open knot vector  $\Xi$  with end knots located at  $a$  and  $b$  (with  $b > a$ ) and with *equispaced* and *non-repeated* interior knots. Because the interior knots are distinct, the functions in this space attain maximal continuity at interior knots. That is,  $K(n, k, a, b) \subset C^{k-1}(a, b)$ .
- $K_{per}(n, k, a, b)$  is the periodic spline space of dimension  $n$  and degree  $k$  corresponding to the open knot vector  $\Xi$  with end knots located at  $a$  and  $b$  and with *equispaced* and *non-repeated* interior knots, subject to periodic boundary conditions of maximal continuity. Namely, if  $u \in K_{per}(n, k, a, b)$ , then

$$D^{(i)}u(a) = D^{(i)}u(b), \quad \forall i = 1, 2, \dots, k - 1. \quad (4)$$

This space is known as the space of *uniform periodic splines*. Maximal order of continuity at all knots is attained in this case.

- $P(n, p, a, b)$  is the B-spline space of dimension  $n$  and degree  $p$  corresponding to the open knot vector  $\Xi$  with end knots located at  $a$  and  $b$ ,  $b > a$ , and with *equispaced* interior knots, each of which is repeated  $p - 1$  times. This is a space of *standard* finite element functions of degree  $p$  that are  $C^0$ -continuous at knots.
- $\mathcal{P}(n, a, b)$  is the B-spline space of dimension  $n$  and degree  $n - 1$  corresponding to the open knot vector  $\Xi$  with end knots located at  $a$  and  $b$ ,  $b > a$ , and with no interior knots. This is a space of global polynomials of degree  $n - 1$ .

In this paper, we define the *k-version of the isogeometric finite element method* or, in short, the *k-method* as the analysis method exploiting full continuity of the basis functions across distinct knots (and hence results from knot vectors with non-repeated interior knots). Alternatively, we define the *classical finite element method* as the analysis method where only  $C^0$ -continuity is enforced across interior knots. With these definitions, we see that the spaces  $K(n, k, a, b)$  and  $K_{per}(n, k, a, b)$  correspond to the *k-method* while the space  $P(n, p, a, b)$  corresponds to the classical finite element method of degree  $p$ . The space  $\mathcal{P}(n, a, b)$  corresponds to the *spectral method* or the *p-version of the finite element method* and is a special case of both the classical finite element and *k-methods*, the case where no interior knots exist. Examples of these spaces are illustrated in Figure 1.

### 3 Function spaces

In this section, we introduce a number of function spaces which arise in the study of elliptic partial differential equations. Solutions to such equations often live in these function spaces, depending of course on the regularity of the underlying problem and associated boundary conditions.

#### 3.1 Sobolev spaces

Let  $\Omega \subset \mathbb{R}$  be an open domain. For an integer  $m \geq 0$ , we use the notation

$$H^m(\Omega) = \{u \in L^2(\Omega) : D^\alpha u \in L^2(\Omega) \text{ for all } \alpha = 0, \dots, m\}. \quad (5)$$

The Sobolev space  $H^m(\Omega)$  is a Hilbert space with inner-product

$$(u, v)_{H^m(\Omega)} = \sum_{\alpha=0}^m (D^\alpha u, D^\alpha v)_{L^2(\Omega)} \quad (6)$$

and induced-norm  $\|u\|_{H^m(\Omega)} = (u, u)_{H^m(\Omega)}^{1/2}$ . By the Rellich-Kondrachov theorem,  $H^k(\Omega)$  is dense and compactly embedded in  $H^j(\Omega)$  for  $j < k$ . Throughout this paper, we will use the notation

$$B^m(\Omega) = \{u \in H^m(\Omega) : \|u\|_{H^m(\Omega)} \leq 1\}, \quad (7)$$

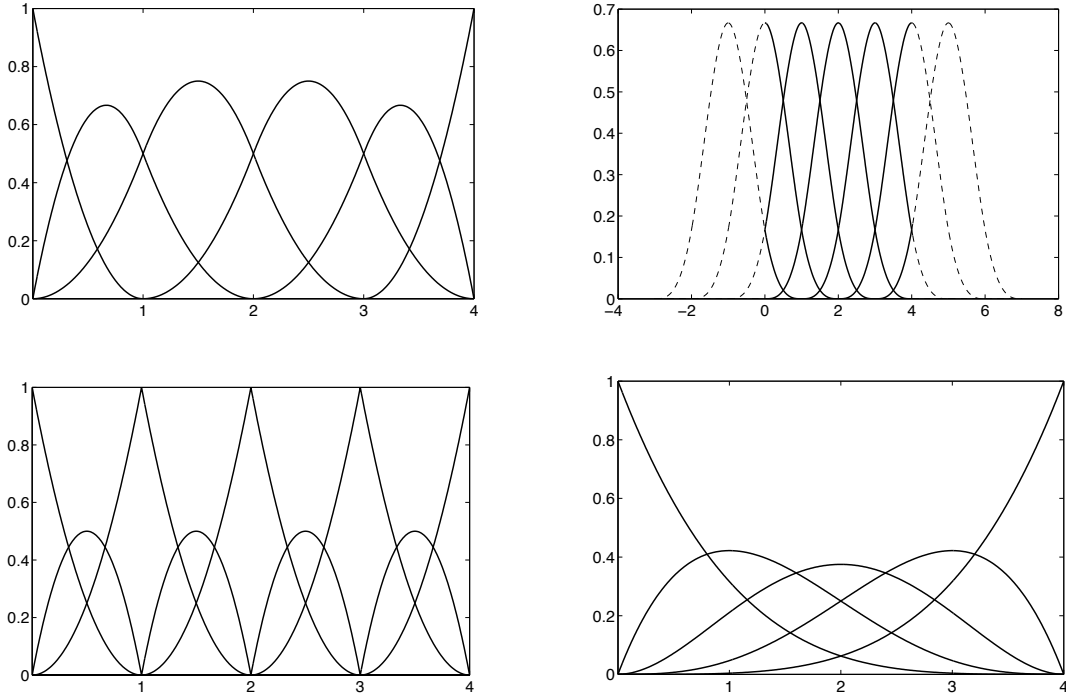


Figure 1: *Top Left:* The B-spline space  $K(6, 2, 0, 4)$ . *Top Right:* The uniform periodic spline space  $K_{per}(4, 3, 0, 4)$ . *Bottom Left:* The B-spline space  $P(9, 2, 0, 4)$ . *Bottom Right:* The B-spline space  $\mathcal{P}(5, 0, 4)$ .

$$\tilde{B}^m(\Omega) = \{u \in H^m(\Omega) : \|D^m u\|_{L^2(\Omega)} \leq 1.\} \quad (8)$$

Note that  $B^m(\Omega)$  is the unit ball of  $H^m(\Omega)$ . We will find that the set  $\tilde{B}^m(\Omega)$  is well-suited to theoretical analysis while the unit ball  $B^m(\Omega)$  is amenable to numerics.

Sobolev spaces are among the most common encountered while studying elliptic boundary value problems. Results such as the elliptic regularity theorem state that suitable weak solutions to elliptic problems live in higher-order Sobolev spaces, so it is important to understand approximability in terms of such spaces.

### 3.2 Periodic Sobolev spaces

To begin, recall that by the Sobolev embedding theorems,  $H^m(0, 2\pi) \subset C^{m-1}([0, 2\pi])$ . Hence, for an integer  $m \geq 0$ , we may define the periodic Sobolev space

$$H_{per}^m(0, 2\pi) = \{u \in H^m(0, 2\pi) : D^i u(0) = D^i u(2\pi) \text{ for } i = 0, 1, \dots, m-1\}. \quad (9)$$

Further, we will use the notation

$$B_{per}^m(0, 2\pi) = \{u \in H_{per}^m(0, 2\pi) : \|u\|_{H^m(0, 2\pi)} \leq 1\} \quad (10)$$

and

$$\tilde{B}_{per}^m(0, 2\pi) = \{u \in H_{per}^m(0, 2\pi) : \|D^m u\|_{L^2(0, 2\pi)} \leq 1\}. \quad (11)$$

We know  $H_{per}^m(0, 2\pi)$  is a complete subspace of  $H^m(0, 2\pi)$ . Hence, it is a Hilbert space equipped with the inner product  $(u, v)_{H^m(0, 2\pi)}$ . Furthermore, we have that  $H_{per}^k(0, 2\pi)$  is dense and compactly embedded in  $H_{per}^j(0, 2\pi)$  for  $j < k$ . Note that  $H_{per}^0(0, 2\pi) = L^2(0, 2\pi)$ .

Periodic Sobolev spaces, while not as common as Sobolev spaces, appear in a number of applications. Common applications where such spaces are employed include wave propagation and turbulence, two areas where  $k$ -methods have shown much promise. We shall demonstrate later in this paper that  $k$ -methods exhibit good behavior when approximating functions from these spaces.

### 3.3 Weighted Sobolev spaces

The study of weighted Sobolev spaces has become increasingly popular in the numerical analysis community. Their use has been of particular interest to those employing the classical  $p$ - and  $hp$ -refinement strategies [6, 7, 10, 30, 17]. Weighted Sobolev spaces are constructed to allow functions with singularities in their domain. As such, they are a natural setting for solutions to problems with corners [3] and non-smooth boundaries (e.g. the ubiquitous L-shaped domain). Since such solutions do not live in higher-order classical Sobolev spaces, we cannot use classical theoretical results to characterize the convergence behavior of finite element approximations. Instead, alternative spaces must be sought out, and weighted Sobolev spaces are a prime candidate for such a task. Approximation theory and numerical results have shown that global polynomials have good approximation behavior for weighted Sobolev spaces when the weight is a measure of the distance from the boundary.

Let  $\alpha \in \mathbb{R}$  such that  $\alpha > -1$ . Let

$$\rho_\alpha(x) = (1 - x^2)^\alpha. \quad (12)$$

We define  $L_\alpha^2(-1, 1)$  to be the space of measurable functions which are  $L^2$ -integrable with respect to the measure  $\rho_\alpha(x)dx$ . That is, if  $D'(-1, 1)$  is the space of distributions,

$$L_\alpha^2(-1, 1) = \left\{ u \in D'(-1, 1) : \|u\|_{L_\alpha^2(-1, 1)} = \left( \int_{-1}^1 |u(x)|^2 \rho_\alpha(x) dx \right)^{1/2} < +\infty \right\}. \quad (13)$$

$L_\alpha^2(-1, 1)$  is a Hilbert space equipped with the inner product

$$(u, v)_{L_\alpha^2(-1, 1)} = \int_{-1}^1 u(x)v(x)\rho_\alpha(x)dx. \quad (14)$$

We note  $L_0^2(-1, 1) = L^2(-1, 1)$ .

Let  $m \geq 0$  be an integer such that  $\alpha - m > -1$ . We define the Jacobi-weighted Sobolev space  $V_\alpha^m(-1, 1)$  by

$$V_\alpha^m(-1, 1) = \left\{ u \in D'(-1, 1) : \|u\|_{V_\alpha^m(-1, 1)} = \left( \sum_{k=0}^m \|D^k u\|_{L_{\alpha+k-m}^2(-1, 1)}^2 \right)^{1/2} < +\infty \right\}, \quad (15)$$

equipped with the inner product

$$(u, v)_{V_\alpha^m(-1, 1)} = \sum_{k=0}^m (D^k u, D^k v)_{L_{\alpha+k-m}^2(-1, 1)}. \quad (16)$$

The spaces  $V_{\alpha+k}^k(-1, 1)$  are compactly embedded and dense in  $V_{\alpha+j}^j(-1, 1)$  for  $j < k$  (see [19] for a proof), and the spaces  $V_k^k(-1, 1)$  are the well-known Legendre-weighted Sobolev spaces. Finally, we denote

$$B_w^{m,\alpha}(-1, 1) = \{u \in V_\alpha^m(-1, 1) : \|u\|_{V_\alpha^m(-1,1)} \leq 1\}. \quad (17)$$

to be the unit ball of the Jacobi-weighted Sobolev space  $V_\alpha^m(-1, 1)$ .

We immediately see that the Jacobi-weighted Sobolev spaces allow for singularities at the points -1 and 1. For example, the function  $\arcsin(x)$ , whose derivative is  $\frac{1}{\sqrt{1-x^2}}$ , lives in  $V_1^1(-1, 1)$  but not in  $H^1(-1, 1)$ . Further, functions of the form  $(1-x)^a(1+x)^b$  with  $-\frac{1}{2} < a, b < 1$ , one-dimensional models of solutions encountered in multi-dimensional linear elasticity boundary value problems posed on polyhedral domains, also live in certain Jacobi-weighted Sobolev spaces. The benefit of studying Jacobi-weighted Sobolev spaces is thus apparent.

## 4 Theory of $n$ -widths and sup-infs

When investigating the effectiveness of a Galerkin or Petrov-Galerkin method, we must first ask how well our chosen basis can represent the exact solution. This question belongs to the realm of approximation theory. In this section, we introduce terminology and concepts to assess the effectiveness of spline-based finite element methods.

### 4.1 Basic terminology

Let  $X$  be a normed linear space with norm  $\|\cdot\|_X$ , and let  $X_n$  be any  $n$ -dimensional subspace of  $X$ . For each  $x \in X$ , we define  $E(x, X_n; X)$  to be the *distance* of the  $n$ -dimensional subspace of  $X_n$  from  $x$ , namely

$$E(x, X_n; X) = \inf_{y_n \in X_n} \|x - y_n\|_X. \quad (18)$$

The concept of distance is illustrated in Figure 2. If there exists a  $y^* \in X_n$  for which  $E(x, X_n; X) = \|x - y^*\|_X$ , then  $y^*$  is called the *best approximation* to  $x$  from  $X_n$ . If  $X$  is a Hilbert space, then  $y^*$  exists and is uniquely defined. Using the finite element method for a symmetric elliptic partial differential equation, one obtains the best approximation in terms of the energy norm. Hence, it is of importance to understand how large the quantity  $E(x, X_n; X)$  can become.

We are not usually interested in just the distance of  $X_n$  from some arbitrary  $x \in X$ ; instead, we are interested in how well the space approximates a subset  $A$  of  $X$ . To this end, we define  $E(A, X_n; X)$  to be the *deviation* of  $A \subset X$  from  $X_n$ , namely

$$E(A, X_n; X) = \sup_{x \in A} \inf_{y_n \in X_n} \|x - y_n\|_X. \quad (19)$$

The notion of deviation is illustrated in Figure 3. We shall also refer to  $E(A, X_n; X)$  as the *sup-inf* for  $A$  and  $X_n$ . The sup-inf gives us a measure of how well an  $n$ -dimensional space  $X_n$  approximates the “worst” member  $x \in A$ .

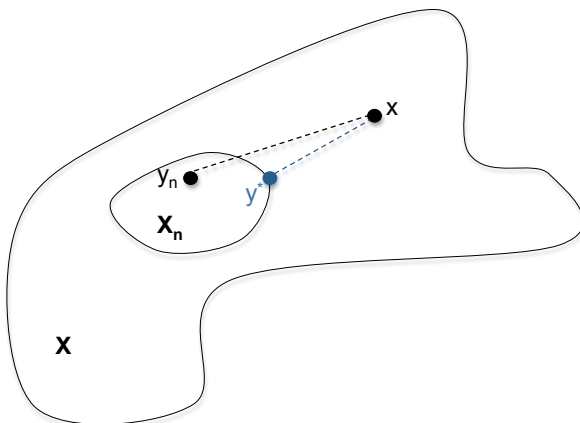


Figure 2: The distance of  $X_n$  from a point  $x \in X$ . In this particular case,  $y^*$  is the best approximation.

Given two  $n$ -dimensional subspaces  $X_n$  and  $Y_n$  of  $X$ , we consider the *comparison ratio*

$$\kappa(A, X_n, Y_n; X) = \frac{E(A, X_n; X)}{E(A, Y_n; X)} \quad (20)$$

in terms of which we can assess the effectiveness of  $X_n$  as compared to  $Y_n$  in approximating the set  $A$  (as introduced by Babuška *et al.* in [4]). If  $\kappa \approx 1$ , we have no strong reason to prefer one subspace over the other. On the other hand, if  $\kappa \ll 1$ , we prefer  $X_n$ , and if  $\kappa \gg 1$ , we prefer  $Y_n$ .

The above criterion is useful for comparing the approximation properties of two spaces, but we are often more interested in comparing multiple spaces. A natural question to ask is how an  $n$ -dimensional subspace  $X_n \subset X$  compares with all other  $n$ -dimensional subspaces of  $X$ . This question can be answered with the notion of  *$n$ -width*, first proposed by Kolmogorov [23]. The Kolmogorov  $n$ -width is defined as

$$d_n(A; X) = \inf \{E(A, X_n; X) : X_n \text{ is an } n\text{-dimensional subspace of } X\} \quad (21)$$

or, equivalently,

$$d_n(A; X) = \inf_{\substack{X_n \subset X \\ \dim X_n = n}} \sup_{x \in A} \inf_{y_n \in X_n} \|x - y_n\|_X. \quad (22)$$

An  $n$ -dimensional subspace  $\tilde{X}_n \subset X$  is said to be *optimal* if

$$E(A, \tilde{X}_n; X) = d_n(A; X). \quad (23)$$

Given a specific  $n$ -dimensional subspace  $X_n \subset X$ , we can now assess its effectiveness by considering the *optimality ratio*

$$\Lambda(A, X_n; X) \equiv \frac{E(A, X_n; X)}{d_n(A; X)} = \frac{E(A, X_n; X)}{E(A, \tilde{X}_n; X)}. \quad (24)$$

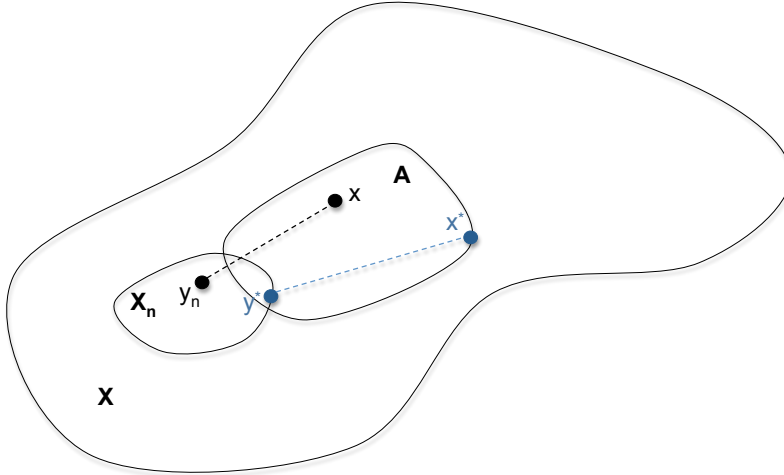


Figure 3: The deviation or sup-inf of  $X_n$  from a set  $A \subset X$ . In this particular case, the sup-inf is achieved with the two points  $x^* \in A$ ,  $y^* \in X_n$ . That is,  $E(A, X_n; X) = \|x^* - y^*\|_X$ .

We see that the ratio  $\Lambda$  compares  $X_n$  with the optimal subspace, and therefore  $\Lambda \geq 1$ . It is a rare occasion that  $\Lambda = 1$ , and much research has been devoted to the search for optimal subspaces. In fact, it is often impossible to obtain  $d_n(A; X)$  and determine the existence of optimal subspaces. If we restrict ourselves to a Hilbert space setting, however, we obtain a variational tool by which we can calculate  $d_n(A; X)$  and a corresponding optimal subspace.

**Remark 4.1.** In general, we may not know precisely where the solution to a partial differential equation lies (that is, we may not know a space  $A$  where  $x$  is *a priori*), but we may know several candidate spaces where the solution may be. By analyzing optimality ratios for these different spaces, we can evaluate the effectiveness of an approximation space across a broad spectrum of situations. Hence, we can determine if a particular approximation space is “good for all seasons.”

We finish this subsection with one more definition. Let  $X_1, X_2, \dots$  be a sequence of subsets of  $X$  such that  $\dim X_i = i$ . If there exists a constant  $M \in \mathbb{R}$  such that

$$E(A, X_i; X) \leq M d_i(A; X) \tag{25}$$

for every  $i \in \mathbb{N}$ , then the subspaces  $\{X_n\}_{n=1}^{\infty}$  are *asymptotically optimal subspaces*. Much of approximation theory research is spent determining if sequences of subspaces are asymptotically optimal. We feel that it is also important to understand the potential size of  $M$ . For example, if  $M = 10^{100}$ , the asymptotically optimal sequence is probably not desirable for the purposes of approximation.

## 4.2 Characterization of $n$ -widths and sup-infs in a Hilbert space setting

We now restrict ourselves to a Hilbert space setting. In doing so, we obtain a number of powerful results. We present here six theorems, the first four of which will be useful for theoretical calculations while the last two lend themselves to numerical computation.

Let  $H$  be a Hilbert space with inner product  $(u, v)_H$  and induced norm  $\|u\|_H$ . Let  $K : H \rightarrow H$  be a compact linear operator. We define  $B_K$  to be the image of the unit ball of  $H$  under  $K$ :

$$B_K = \{u \in H : u = Kv, v \in H, \|v\|_H \leq 1\}. \quad (26)$$

Suppose  $K$  is the solution operator of a linear partial differential equation. The set  $B_K$  then represents the set of all solutions subject to an appropriately bounded forcing.

We are interested in the quantity

$$d_n(B_K; H) = \inf_{\substack{X_n \subset H \\ \dim X_n = n}} \sup_{u \in B_K} \inf_{v_n \in X_n} \|u - v_n\|_H. \quad (27)$$

Before proceeding, recall the following classical duality result. It will be instrumental in arriving at a mechanism for computing (27).

**Lemma 4.1.** *Let  $X_n$  denote an  $n$ -dimensional subspace of  $H$  and  $v \in H$ . Then*

$$\inf_{v_n \in X_n} \|v - v_n\|_H = \sup_{\substack{f \in H \\ f \neq 0 \\ (f, X_n)_H = 0}} \frac{(v, f)_H}{\|f\|_H} \quad (28)$$

where  $(f, X_n)_H = 0$  indicates that  $f$  is orthogonal to each element  $v_n \in X_n$ .

*Proof.* Let  $\pi_n$  be the  $H$ -projection onto  $X_n$ . That is, for every  $u \in H$ , let  $\pi_n u$  be the unique member of  $X_n$  such that

$$\|u - \pi_n u\|_H = \inf_{v_n \in X_n} \|u - v_n\|_H. \quad (29)$$

Recall from functional analysis that  $\pi_n$  is a unique bounded self-adjoint linear surjection. Then, one can write

$$\begin{aligned} \inf_{v_n \in X_n} \|v - v_n\|_H &= \|(I - \pi_n)v\|_H \\ &= \sup_{\substack{f \in H \\ \|f\|_H = 1}} ((I - \pi_n)v, f)_H \\ &= \sup_{\substack{f \in H \\ \|f\|_H = 1}} (v, (I - \pi_n)f)_H \\ &= \sup_{\substack{f \in H \\ \|f\|_H = 1 \\ (f, X_n)_H = 0}} (v, f)_H. \end{aligned} \quad (30)$$

Result (28) follows.  $\square$

The next theorem characterizes the quantity (27) and an associated optimal subspace.

**Theorem 4.1.** *Let*

$$\mu_1 \geq \mu_2 \geq \dots \searrow +0, \quad \psi_1, \psi_2, \dots, \quad (31)$$

*denote the eigenvalues and eigenvectors of the self-adjoint, non-negative, compact operator  $KK^*$ . Then for  $n = 1, 2, \dots$ ,*

$$d_n(B_K; H) = \mu_{n+1}^{1/2} \quad (32)$$

*and*

$$\tilde{X}_n = \text{span} \{ \psi_1, \dots, \psi_n \} \quad (33)$$

*is an optimal subspace for  $d_n(B_K; H)$ .*

*Proof.* By definition,

$$d_n(B_K; H) = \inf_{\substack{X_n \subset H \\ \dim X_n = n}} \sup_{\substack{v \in H \\ \|v\|_H = 1}} \inf_{v_n \in X_n} \|Kv - v_n\|_H. \quad (34)$$

By Lemma 4.1,

$$\inf_{v_n \in X_n} \|Kv - v_n\|_H = \sup_{\substack{f \in H \\ f \neq 0 \\ (f, X_n)_H = 0}} \frac{(Kv, f)_H}{\|f\|_H} \quad (35)$$

for every  $v \in H$ . It follows that

$$\begin{aligned} d_n(B_K; H) &= \inf_{\substack{X_n \subset H \\ \dim X_n = n}} \sup_{\substack{v \in H \\ \|v\|_H = 1}} \sup_{\substack{f \in H \\ f \neq 0 \\ (f, X_n)_H = 0}} \frac{(Kv, f)_H}{\|f\|_H} \\ &= \inf_{\substack{X_n \subset H \\ \dim X_n = n}} \sup_{\substack{f \in H \\ f \neq 0 \\ (f, X_n)_H = 0}} \sup_{\substack{v \in H \\ \|v\|_H = 1}} \frac{(v, K^*f)_H}{\|f\|_H} \\ &= \inf_{\substack{X_n \subset H \\ \dim X_n = n}} \sup_{\substack{f \in H \\ f \neq 0 \\ (f, X_n)_H = 0}} \frac{\|K^*f\|_H}{\|f\|_H} \\ &= \left[ \inf_{\substack{X_n \subset H \\ \dim X_n = n}} \sup_{\substack{f \in H \\ f \neq 0 \\ (f, X_n)_H = 0}} \frac{(KK^*f, f)_H}{(f, f)_H} \right]^{1/2}. \end{aligned} \quad (36)$$

This final expression is the well-known Rayleigh-Ritz characterization of the square root of the  $(n+1)$ st largest eigenvalue ( $\mu_{n+1}^{1/2}$ ) of  $KK^*$ , and the infimum in the above expression is obtained by the choice  $\text{span}\{\psi_1, \dots, \psi_n\}$ . Results (32) and (33) follow.  $\square$

**Example 4.1. (Sturm-Liouville Problems)** Consider the following second-order regular Sturm-Liouville problem:

$$-(pu')' + qu = f \quad \text{on} \quad (a, b), \quad (37)$$

$$\alpha_1 u(a) - \alpha_2 u'(a) = 0, \quad (38)$$

$$\beta_1 u(b) + \beta_2 u'(b) = 0, \quad (39)$$

where  $(\cdot)'$  denotes a derivative operator,  $f \in L^2(a, b)$ ,  $p \in C^1[a, b]$ ,  $p > 0$ ,  $q \in C^0[a, b]$ ,  $q \geq 0$ , and  $\alpha_1, \alpha_2, \beta_1, \beta_2 > 0$ . The solution  $u$  is unique and can be written as

$$u(x) = (Kf)(x) = \int_a^b G(x, y)f(y)dy, \quad (40)$$

where  $G(x, y)$  is the Green's function and  $K$  is the solution (i.e. Green's) operator. Noting that  $K : L^2(a, b) \rightarrow L^2(a, b)$  is a compact operator, we see Theorem 4.1 yields optimal discrete spaces for the approximation of the solution of the Sturm-Liouville problem.

There are also optimal subspaces other than the ones given in (33). In fact, for a number of cases, optimal subspaces can be selected to be spline subspaces. We will discuss a number of these later on in this paper. For compact operators that can be characterized as the action of an integrable kernel (as in Example 4.1), we have another mechanism through which we can arrive at optimal subspaces. In particular, for general integral operators with a non-degenerate totally positive kernel (see [24] for definition) we have the following theorem.

**Theorem 4.2.** *Let  $K(x, y)$  be a non-degenerate totally positive kernel on  $(a, b) \times (a, b)$  and let the operator  $K : L^2(a, b) \rightarrow L^2(a, b)$  be defined as*

$$(Kf)(x) = \int_a^b K(x, y)f(y)dy, \quad \forall f \in L^2(a, b). \quad (41)$$

*By construction, the operator  $K$  is compact. Let  $a < \xi_1 < \xi_2 < \dots < \xi_n < b$  denote the zeros of the  $(n + 1)^{\text{st}}$  eigenvector of  $K$ . Then the following subspace is also optimal for  $d_n(B_K; L^2(a, b))$ :*

$$\hat{X}_n = \text{span}\{K(\cdot, \xi_1), K(\cdot, \xi_2), \dots, K(\cdot, \xi_n)\}. \quad (42)$$

*Proof.* The proof is due to Melkman and Micchelli. See [24].

The next theorem characterizes  $n$ -widths and associated optimal subspaces for sets which may be described as the direct sum of a finite-dimensional space and the image of a compact operator. Such sets are of direct relevance to Hilbert spaces without boundary conditions.

**Theorem 4.3.** *Let  $K(x, y)$  and  $K$  be as in Theorem 4.2. Let*

$$B_K^r = \{v(x) : v(x) = \sum_{i=1}^r a_i k_i(x) + (Kf)(x), f \in L^2(a, b), a_i \in \mathbb{R}\} \quad (43)$$

such that  $k_i(x)$  and  $K(x, y)$  satisfy certain non-degenerate total positivity requirements (see [24] for details). Then:

$$d_n(B_K^r; L^2(a, b)) = \begin{cases} \infty, & n < r, \\ \mu_{n-r+1}^{1/2}, & n \geq r, \end{cases} \quad (44)$$

and the following spaces are optimal for  $d_n(B_K^r; L^2(a, b))$ :

$$\tilde{X}_n = \text{span} \{k_1, k_2, \dots, k_r, \psi_1, \psi_2, \dots, \psi_{n-r}\} \quad (45)$$

and

$$\hat{X}_n = \text{span} \{k_1, k_2, \dots, k_r, K(\cdot, \xi_1), K(\cdot, \xi_2), \dots, K(\cdot, \xi_{n-r})\}. \quad (46)$$

*Proof.* See [24].

**Example 4.2. (Optimality of Splines)** It is well-known that any function  $v(x) \in \tilde{B}^s(0, 1)$  can be written as

$$v(x) = \sum_{i=0}^{s-1} \frac{D^i v(0)}{i!} x^i + \frac{1}{(s-1)!} \int_0^1 (x-y)_+^{s-1} f(y) dy, \quad (47)$$

where  $f = D^s v \in L^2(0, 1)$  and

$$(z)_+ = \begin{cases} z & \text{if } z > 0 \\ 0 & \text{otherwise} \end{cases}. \quad (48)$$

Immediately applying Theorem 4.3, one finds that the space

$$\text{span} \{1, x, x^2, \dots, x^{s-1}, (x - \xi_1)_+^{s-1}, (x - \xi_2)_+^{s-1}, \dots, (x - \xi_{n-s})_+^{s-1}\} \quad (49)$$

is an optimal subspace for  $d_n(\tilde{B}^s(0, 1), L^2(0, 1))$ . Above, as usual,  $0 < \xi_1 < \dots < \xi_{n-s} < 1$  denote the zeros of the  $(n-s+1)^{st}$  eigenvector of operator  $K$  defined by

$$Kf(x) = \int_0^1 (x-y)_+^{s-1} f(y) dy. \quad (50)$$

One finds that the space given by (49) is the space of B-splines of order  $s-1$  corresponding to the open knot vector  $\Xi = \{0, \dots, 0, \xi_1, \dots, \xi_{n-s}, 1, \dots, 1\}$  (that is, the space  $S(n, s-1, \Xi)$ ). These knot locations are fixed for every choice of  $s$  and  $n$  and are, in general, non-uniform. However, these locations are symmetric relative to the midpoint of  $(0,1)$ . These locations are generally hard to obtain since to the best of the authors' knowledge explicit closed-form expressions for the eigenfunctions, and, as a result, their zeros, are not known. It will be shown in the numerical computations section of this paper that choosing a uniform partition of the knot vector leads to nearly optimal approximation properties of the resultant B-spline spaces.

Our next result pertains to functions induced by a  $2\pi$ -periodic continuous kernel.

**Theorem 4.4.** *Let  $D(x)$  be a real  $2\pi$ -periodic function with the following Fourier series representation:*

$$D(x) = \sum_{n=-\infty}^{\infty} a_n e^{inx}, \quad (51)$$

where  $i = \sqrt{-1}$  and  $|a_n| = |a_{-n}|$ . Suppose  $D(x)$  satisfies certain positivity conditions as outlined in Chapter 6 of [26] (known collectively as Property B). Further define

$$B_D = \{v(x) : v(x) = c + D * f(x), f \in L^2(0, 2\pi), \|f\|_{L^2(0, 2\pi)} \leq 1, f \perp 1, c \in \mathbb{R}\} \quad (52)$$

where

$$D * f(x) = \int_0^{2\pi} D(x - y)f(y)dy. \quad (53)$$

Then,

$$d_0(B_D; L^2(0, 2\pi)) = \infty, \quad (54)$$

$$d_{2n-1}(B_D; L^2(0, 2\pi)) = d_{2n}(B_D; L^2(0, 2\pi)) = |a_n|, \quad n \geq 1, \quad (55)$$

and two corresponding optimal subspaces are

$$\tilde{X}_{2n-1} = \text{span}\{1, \cos(x), \sin(x), \dots, \cos((n-1)x), \sin((n-1)x)\} \quad (56)$$

and

$$\hat{X}_{2n} = \left\{ v(x) : v(x) = b_0 + \sum_{j=1}^{2n} b_j D(x - (j-1)\pi/n) \text{ such that } \sum_{j=1}^{2n} b_j = 0 \right\}. \quad (57)$$

*Proof.* The proof is due to Pinkus. See [26].

**Example 4.3. (Optimality of Periodic Splines)** Any function in the space  $\tilde{B}_{per}^s(0, 2\pi)$  may be written as

$$v(x) = c + \frac{1}{\pi} \int_0^{2\pi} \mathcal{B}_s(x - y)f(y)dy, \quad (58)$$

where  $f = D^s v \in L^2(0, 2\pi)$ ,  $c = \int_0^{2\pi} v(y)dy$ ,  $\int_0^{2\pi} f(y)dy = 0$ , and  $\mathcal{B}_s$  is defined by

$$\mathcal{B}_s(x) = \sum_{n=1}^{\infty} \frac{\cos(nx - (s\pi/2))}{n^s}. \quad (59)$$

It is easy to establish that  $\mathcal{B}_s$  is a  $2\pi$ -periodic spline (the so-called Bernoulli monospline) of order  $s$  that is  $C^{s-2}$  at the point 0 and has polynomial representation over the interval  $[0, 2\pi)$  (see [26] for a further discussion). Invoking Theorem 4.4, one finds that for  $s > 1$ ,

$$d_0(\tilde{B}_{per}^s(0, 2\pi); L^2(0, 2\pi)) = \infty, \quad (60)$$

$$d_{2n-1}(\tilde{B}_{per}^s(0, 2\pi); L^2(0, 2\pi)) = d_{2n}(\tilde{B}_{per}^s(0, 2\pi); L^2(0, 2\pi)) = n^{-s}, \quad n \geq 1, \quad (61)$$

and

$$\hat{X}_{2n} = \left\{ v(x) : v(x) = b_0 + \sum_{j=1}^{2n} b_j \mathcal{B}_s(x - (j-1)\pi/n) \text{ such that } \sum_{j=1}^{2n} b_j = 0 \right\} \quad (62)$$

is an associated optimal subspace for  $d_{2n} \left( \tilde{B}_{per}^s(0, 2\pi); L^2(0, 2\pi) \right)$ . With some quick analysis, one further finds that  $\hat{X}_{2n} = K_{per}(2n, s-1, 0, 2\pi)$ . This result is quite powerful. Uniform periodic spline spaces are very easy to construct, and this result reveals that they are in fact optimal. Later on in this paper, we will see through the use of numerics a robustness result to complement this accuracy result.

While Theorems 4.1 through 4.4 are useful for the theoretical derivation of  $n$ -widths and corresponding subspaces (as illustrated in Examples 4.1 through 4.3), it is in general not possible to explicitly represent a function class of interest as the image of a compact operator. Furthermore, calculating the eigenvalues and eigenfunctions of a compact operator is a cumbersome and difficult task, and we are also often interested in the computation of sup-infs for particular approximation spaces. In what follows, we give a variational framework that gives a characterization of  $n$ -widths that is amenable to direct computation and allows for a direct computation of the approximation power of any finite-dimensional space in terms of the sup-inf and optimality ratio.

Let  $V$  be a Hilbert space with inner product  $(u, v)_V$  and induced norm  $\|u\|_V$ . Let  $V$  be dense and compactly embedded in  $H$ . We define  $B_V$  to be the unit ball of  $V$ :

$$B_V = \{u \in V : \|u\|_V \leq 1\}. \quad (63)$$

We are now interested in the quantity

$$d_n(B_V; H) = \inf_{\substack{X_n \subset H \\ \dim X_n = n}} \sup_{u \in B_V} \inf_{v_n \in X_n} \|u - v_n\|_H \quad (64)$$

whose value and corresponding optimal subspace can be characterized by the eigenpairs of the following eigenvalue problem:

$$\begin{cases} \lambda \in \mathbb{R}, & u \in V, & u \neq 0, \\ (u, v)_H = \lambda(u, v)_V, & \text{for all } v \in V. \end{cases} \quad (65)$$

Since  $V$  is compact in  $H$ , we know problem (65) has eigenvalues and orthogonal eigenvectors

$$\lambda_1 \geq \lambda_2 \geq \dots \searrow +0, \quad u_1, u_2, \dots, \quad (66)$$

where the eigenvectors are chosen to satisfy

$$(u_i, u_j)_H = \lambda_i (u_i, u_j)_V = \lambda_i \delta_{ij}. \quad (67)$$

We now prove a fundamental theorem on  $n$ -widths. It was also used for the computations in [4], and an alternative derivation may be found in [2].

**Theorem 4.5.** For  $n = 1, 2, \dots$ ,

$$d_n(B_V; H) = \lambda_{n+1}^{1/2} \quad (68)$$

and

$$\tilde{X}_n = \text{span} \{u_1, \dots, u_n\} \quad (69)$$

is an optimal subspace for  $d_n(B; H)$ .

*Proof.* For  $v \in H$ , we let  $L_v \in V^*$  be the functional defined by

$$L_v(w) = (w, v)_H, \quad \text{for all } w \in V. \quad (70)$$

By the Riesz Representation theorem, there exists a unique  $z_v \in V$  such that

$$(w, z_v)_V = L_v(w), \quad \text{for all } w \in V. \quad (71)$$

We define the operator  $S : H \rightarrow V$  by  $Sv = z_v$  for all  $v \in H$ . One can easily show  $S$  is a linear, bounded operator which maps from  $H$  into  $V$ . Let  $T : H \rightarrow H$  be defined by

$$Tv = Sv \quad (72)$$

for all  $v \in H$ . Since  $V$  is compact in  $H$ , it follows that  $T$  is a compact operator, and one can also show  $T$  is self-adjoint and positive. We then know  $T$  has eigenvalues and eigenvectors

$$\mu_1 \geq \mu_2 \geq \dots \searrow +0, \quad \psi_1, \psi_2, \dots, \quad (73)$$

with  $\mu_i > 0$ , and it is easy to show that  $\mu_i = \lambda_i$  and  $\psi_i = u_i$  in Equation (66).

From basic Hilbert space theory, we know  $T$  has a unique positive, self-adjoint square root  $T^{1/2}$ . Further, one can show  $T^{1/2}$  is also self-adjoint for the inner-product  $(\cdot, \cdot)_V$ . We then have

$$\|T^{1/2}u\|_V^2 = (Tu, u)_V = \|u\|_H^2 \quad \text{for all } u \in V \quad (74)$$

and, by density,  $\|T^{1/2}u\|_V = \|u\|_H$  for all  $u \in H$ . It follows that  $B_V$  is the image of the unit ball of  $H$  under  $T^{1/2}$ . Results (68) and (69) follow from Theorem 4.1.  $\square$

**Example 4.4. (Optimality of Polynomials in Jacobi-weighted Spaces)** The space of polynomials  $\mathcal{P}(n, -1, 1)$  is an optimal subspace for the  $n$ -width  $d_n(B_w^{m, m+\alpha}(-1, 1); L_\alpha^2(-1, 1))$  as the Jacobi polynomials are the corresponding eigenvectors of (69).

We have so far characterized  $n$ -widths and optimal subspaces in terms of the eigenpairs of certain eigenvalue problems. We can employ a similar technique to compute sup-infs. Let  $X_n$  be an  $n$ -dimensional subspace of  $H$ . Let  $\pi_n$  be the  $H$ -projection onto  $X_n$ . Consider the eigenvalue problem

$$\begin{cases} \tilde{\lambda} \in \mathbb{R}, \tilde{u} \in V, \tilde{u} \neq 0, \\ ((I - \pi_n)\tilde{u}, (I - \pi_n)v)_H = \tilde{\lambda}(\tilde{u}, v)_V, \text{ for all } v \in V. \end{cases} \quad (75)$$

We know (75) is a well-posed eigenvalue problem (with up to  $n$  zero eigenvalues) whose nonzero eigenvalues satisfy

$$\tilde{\lambda}_1 \geq \tilde{\lambda}_2 \geq \dots \searrow +0. \quad (76)$$

The largest eigenvalue,  $\tilde{\lambda}_1$ , is the Rayleigh quotient characterized by

$$\tilde{\lambda}_1 = \sup_{u \in V} \frac{\|u - \pi_n u\|_H^2}{\|u\|_V^2}. \quad (77)$$

From this expression, we immediately have the following theorem characterizing the sup-inf  $E(B_V, X_n; H)$ .

**Theorem 4.6** *If  $\tilde{\lambda}_1$  is the largest eigenvalue of (75), then*

$$E(B_V, X_n; H) = \tilde{\lambda}_1^{1/2}. \quad (78)$$

Theorems 4.5 and 4.6 provide a variational framework through which we may numerically compute  $n$ -widths and sup-infs. Such a framework is ideal for finite element technologies.

### 4.3 Relation of sup-infs to Galerkin *a priori* error estimates

We finish this section by establishing a relationship between sup-infs and Galerkin *a priori* error estimates. This motivates the computation of  $n$ -widths and sup-infs as a means of assessing the effectiveness of a finite element basis.

Let  $\Omega \subset \mathbb{R}^d$  be an open domain. Let  $B : H^1(\Omega) \times H^1(\Omega) \rightarrow \mathbb{R}$  be a continuous, coercive bilinear functional and  $F \in (H^1(\Omega))^*$ . Consider the variational problem:

Find  $u \in H^1(\Omega)$  such that

$$B(u, v) = F(v), \quad \text{for all } v \in H^1(\Omega). \quad (79)$$

The variational formulation of many linear elliptic second-order partial-differential equations can be written in the form of (79). The Lax-Milgram theorem gives the existence and uniqueness of a weak solution  $u$ , provided that continuity and coercivity of the bilinear form  $B$  holds.

The Galerkin method involves choosing an  $n$ -dimensional subspace  $X_n$  of  $H^1(\Omega)$  with which we will approximate the weak solution. The resulting finite-dimensional problem is:

Find  $u_n \in X_n$  such that

$$B(u_n, v_n) = F(v_n), \quad \text{for all } v_n \in X_n. \quad (80)$$

One can easily show that (80) has a unique solution  $u_n$ , and if  $M$  and  $\gamma$  are the continuity and coercivity constants for  $B$ , we have the inequality

$$\|u - u_n\|_{H^1(\Omega)} \leq \frac{M}{\gamma} \inf_{v_n \in X_n} \|u - v_n\|_{H^1(\Omega)} = \frac{M}{\gamma} E(u, X_n; H^1(\Omega)). \quad (81)$$

The above is the most primitive Galerkin *a priori* error estimate. If our bilinear form is symmetric, we can develop an additional estimate based on the energy norm where the continuity and coercivity constants are both one. The focus of much of the theory of finite elements is to obtain upper bounds on the size of  $E(u, X_n; H^1(\Omega))$ .

Provided that the boundary of  $\Omega$  and parameters of our bilinear form and  $F$  are smooth enough, we can use the elliptic regularity theorem to show our solution  $u$  lives in a higher-order Sobolev space  $H^m(\Omega)$ . We then have the upper bound

$$\|u - u_n\|_{H^1(\Omega)} \leq \frac{M}{\gamma} E(B^m(\Omega), X_n; H^1(\Omega)) \|u\|_{H^m(\Omega)}. \quad (82)$$

The sup-inf  $E(B^m(\Omega), X_n; H^1(\Omega))$  can be computed directly from (78). Traditionally, finite element theorists have instead employed other means to estimate its size (e.g., the Bramble-Hilbert lemma [13]). In fact, employing a Galerkin method to solve the eigenproblem for  $E(B^m(\Omega), X_n; H^1(\Omega))$  requires the use of a finite-dimensional subspace of  $H^m(\Omega)$ . With classical finite element analysis, this is impossible. On, the other hand, the computation can be completed with higher-order continuous functions as in the  $k$ -method.

We feel that the ability to directly compute the sup-inf  $E(B^m(\Omega), X_n; H^1(\Omega))$  with the aid of the  $k$ -method is quite powerful. It allows the finite element theorist to numerically analyze the approximation power of a chosen basis and compare it with other choices. Further, by analyzing trends in  $E(B^m(\Omega), X_n; H^1(\Omega))$ , one can more easily derive theoretical results for finite element spaces. In the following section, we will discuss the numerical computation of sup-infs using Galerkin finite element methods and reveal some results in the context of the classical finite element and  $k$ -methods.

## 5 Numerical approximation results for spline spaces

In this section, we utilize the framework developed in Subsection 4.2 to numerically compute  $n$ -widths and sup-infs for spline spaces in the context of a number of function spaces. Following an in-depth analysis of the  $k$ -method using this framework and the new concept of an optimality surface, we conduct a comparison study between the classical finite element and  $k$ -methods and uncover some interesting results which may help explain some of the recent successes of the  $k$ -method. We finish with a short analysis of the robustness of polynomial approximation using the spectral method.

### 5.1 Galerkin approximation of $n$ -widths and sup-infs

As usual, we assume  $H$  and  $V$  are Hilbert spaces such that  $V$  is dense and compactly embedded in  $H$ ,  $B_V$  is the unit ball of  $V$ , and  $X_n \subset H$  such that  $\dim(X_n) = n$ . We are interested in numerically approximating the  $n$ -width  $d_n(B_V; H)$  and sup-inf  $E(B_V, X_n; H)$ , through which we may then approximate the optimality ratio. We will approximate these quantities using the Galerkin method.

Choose  $X_m \subset V$  such that  $\dim(X_m) = m$ , where  $m \gg n$ . Galerkin approximations to the eigenvalues of (65) and (75) are found by solving the following finite-dimensional eigenproblems:

Find  $u \in X_m$ ,  $\zeta \in \mathbb{R}$  such that

$$(u, v)_H = \zeta (u, v)_V, \quad \text{for } v \in X_m. \quad (83)$$

Find  $\tilde{u} \in X_m$ ,  $\tilde{\zeta} \in \mathbb{R}$  such that

$$((I - \pi_n)\tilde{u}, (I - \pi_n)v)_H = \tilde{\zeta} (\tilde{u}, v)_V, \quad \text{for } v \in X_m. \quad (84)$$

We rewrite (83) and (84) as matrix eigenproblems. Such a form is well-suited for numerical computation as many numerical solvers exist for generalized matrix eigenproblems. We will discuss numerical details for our particular systems shortly.

Assume that  $\{N_i^h\}_{i=1}^n$  and  $(N'_i)_{i=1}^m$  are bases for the spaces  $X_n$  and  $X_m$  respectively. For each  $u \in X_m$ , write  $\mathbf{u} = [u_j]$ , where  $u_j$  is the coefficient of  $u$  with respect to the basis function  $N'_j$ . We define  $\mathbf{H} = [H_{i,j}]$  to be the  $n \times n$  matrix such that

$$H_{i,j} = (N_i^h, N_j^h)_H, \quad (85)$$

$\mathbf{M} = [M_{i,j}]$  and  $\mathbf{K} = [K_{i,j}]$  to be the  $m \times m$  matrices such that

$$M_{i,j} = (N'_i, N'_j)_H \quad \text{and} \quad (86)$$

$$K_{i,j} = (N'_i, N'_j)_V, \quad (87)$$

$\mathbf{T} = [T_{i,j}]$  to be the  $n \times m$  matrix such that

$$T_{i,j} = (N_i^h, N'_j)_H, \quad (88)$$

and  $\tilde{\mathbf{M}} = [\tilde{M}_{i,j}]$  to be the  $m \times m$  matrix such that

$$\tilde{\mathbf{M}} = \mathbf{M} - \mathbf{T}^T \mathbf{H}^{-1} \mathbf{T}. \quad (89)$$

We know that  $\mathbf{K}$  and  $\mathbf{M}$  are positive definite and  $\tilde{\mathbf{M}}$  is positive semi-definite. The generalized matrix eigenproblems

$$\mathbf{M}\mathbf{u} = \zeta \mathbf{K}\mathbf{u} \quad (90)$$

and

$$\tilde{\mathbf{M}}\mathbf{u} = \tilde{\zeta} \mathbf{K}\mathbf{u} \quad (91)$$

are equivalent to (83) and (84). Let

$$\tilde{n} = \dim \left( \text{null} \left( \tilde{\mathbf{M}} \right) \right) = \dim (X_m \cap X_n). \quad (92)$$

Then (90) and (91) have nonzero eigenvalues  $\zeta_1 \geq \dots \geq \zeta_m > 0$  and  $\tilde{\zeta}_1 \geq \dots \geq \tilde{\zeta}_{m-\tilde{n}} > 0$ , respectively. The Galerkin estimates for the  $n$ -width and sup-inf are respectively

$$\begin{aligned} d_n(B_V; H) &\approx \zeta_{n+1}^{1/2}, \\ E(B_V, X_n; H) &\approx \tilde{\zeta}_1^{1/2}. \end{aligned} \quad (93)$$

We finish here with some *a priori* estimates for the error of our approximations. We define the sets

$$U_j = \{u \in V : u \text{ is a generalized eigenvector of (65) corresponding to } \lambda_j, \|u\|_V = 1\} \quad (94)$$

and

$$\tilde{U}_j = \left\{ \tilde{u} \in V : \tilde{u} \text{ is a generalized eigenvector of (75) corresponding to } \tilde{\lambda}_j, \|\tilde{u}\|_V = 1 \right\}. \quad (95)$$

Because of the Rayleigh-Ritz characterization of the eigenvalues of (65) and (75) and their Galerkin counterparts, we further have the inequalities

$$\zeta_j \leq \lambda_j \quad (96)$$

and

$$\tilde{\zeta}_j \leq \tilde{\lambda}_j. \quad (97)$$

These inequalities state that the discrete eigenvalues are smaller or equal in magnitude than the exact eigenvalues. By Theorem 8.3 of [5] and Equations (96) and (97), we obtain the estimates

$$1 \leq \frac{\lambda_{n+1}}{\zeta_{n+1}} \leq C_1 (E(U_{n+1}, X_m; H))^2 + 1 \quad (98)$$

and

$$1 \leq \frac{\tilde{\lambda}_1}{\tilde{\zeta}_1} \leq C_2 \left( E(\tilde{U}_1, X_m; H) \right)^2 + 1 \quad (99)$$

where  $C_1$  is a positive constant which depends on  $H$  and  $V$  and  $C_2$  is a positive constant which depends on  $H$ ,  $V$ , and  $X_n$ . Note that  $C_1$  and  $C_2$  do not depend on  $X_m$ . From these estimates, we immediately have

$$1 \leq \frac{d_n(B_V; H)}{\zeta_{n+1}^{1/2}} \leq (C_1 (E(U_{n+1}, X_m; H))^2 + 1)^{1/2} \quad (100)$$

and

$$1 \leq \frac{E(B_V, X_n; H)}{\tilde{\zeta}_1^{1/2}} \leq \left( C_2 \left( E(\tilde{U}_1, X_m; H) \right)^2 + 1 \right)^{1/2}. \quad (101)$$

Equations (100) and (101) characterize the convergence of our Galerkin method as  $m \rightarrow \infty$ .

## 5.2 A spline-based finite element framework and implementational details

In this paper, we are interested in the case when  $H$  and  $V$  correspond to properly weighted Sobolev spaces and  $X_n$  is a given spline space. Since classical finite elements do not live in higher-order Sobolev spaces, we employ  $k$ -version finite elements to approximate (65) and (75) by the Galerkin method.

In spline-based finite element analysis, elements are interpreted as the span between two consecutive knots. With such a notion, an element-by-element assembly can be conducted

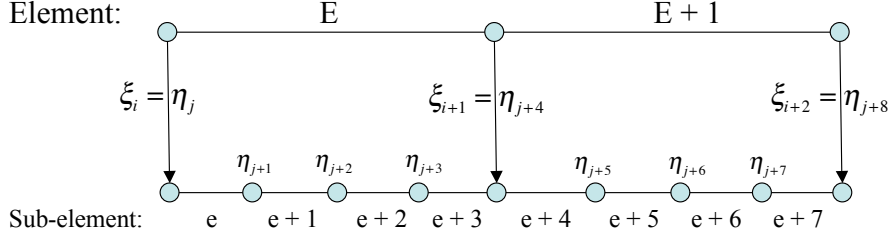


Figure 4: Superconnectivity: The knot vector  $\mathcal{H} = \{\eta_j\}$  for a spline space  $X_m$  is constructed from the knot vector  $\Xi = \{\xi_i\}$  of a spline space  $X_n$ . An element superconnectivity is readily inferred, with parent element  $E$  having children elements  $e$  through  $e + 3$  and parent element  $E + 1$  having children elements  $e + 4$  through  $e + 7$ .

in the usual sense to construct the matrices discussed in the previous subsection. If the knot vector for the trial space  $X_m$  is a simple refinement of the knot vector for the spline space  $X_n$ , an element superconnectivity can be constructed, greatly simplifying the assembly process. This superconnectivity concept is illustrated in Figure 4. By analyzing this figure we see each element corresponding to the knot vector of  $X_m$  is completely contained in a unique element of the knot vector of  $X_n$ . Such a relationship establishes the notion of children elements (the elements corresponding to  $X_m$ ) and parent elements (the elements corresponding to  $X_n$ ). To build our matrices, we then have two nested loops in our assembly process: (1) an outer loop over our parent elements, and (2) an inner loop over the parent’s associated children elements. This structure is especially useful for easy construction of the matrix  $\mathbf{T}$  which couples the spaces  $X_n$  and  $X_m$ .

Since splines have compact support, the matrices  $\mathbf{H}$ ,  $\mathbf{M}$ ,  $\mathbf{K}$ , and  $\mathbf{T}$  have a sparse, banded structure. The matrix  $\tilde{\mathbf{M}}$ , on the other hand, is often fully populated. Hence, it is advantageous to employ algorithms which will allow us never to directly construct  $\tilde{\mathbf{M}}$ . Such a feat could be accomplished through the use of iterative linear solvers within our eigensolver. In fact, an inverse-free preconditioned Krylov subspace symmetric eigensolver specifically designed for systems such as (90) and (91) has been recently introduced by Golub and Ye [18]. We feel that such a solver would be ideal for multi-dimensional computations. However, in one dimension, the matrices are small enough such that direct eigensolvers may be employed effectively.

We employed the QR method for the eigensolves in this paper. In one dimension, the matrix  $\mathbf{K}$  is fast to directly invert due to its tightly banded structure and an explicit expression for the matrix  $\tilde{\mathbf{M}}$  is also easily obtained. Further, we found the QR method to be a robust, stable, and quick method in one dimension.

For the following computations, we utilized  $C^5$  sextic splines for the trial spaces in Galerkin’s method. For each eigenvalue problem, we increased the size  $m$  of the space  $X_m$  until convergence was reached. We found that that for most computations, a sufficient size satisfied the ratio  $\frac{m}{n} \geq 5$ . However, for some of the calculations, a larger  $m$  was necessary. In particular, it was especially difficult to converge some of the results for the case of singular Sobolev spaces. We feel that this might be due to the lack of smoothness associated with these spaces.

### 5.3 Numerically computed optimality surfaces for the $k$ -method

In this subsection, we numerically compute *optimality surfaces* for the  $k$ -method. Given  $n$ , the number of degrees of freedom for a spline space, an optimality surface is a bivariate function of  $s$ , the smoothness of the function space to be approximated, and  $k$ , the polynomial order of the spline space. The optimality surface returns for each  $s$  and  $k$  the optimality ratio for the spline space of order  $k$  in approximating the function space of smoothness  $s$ .

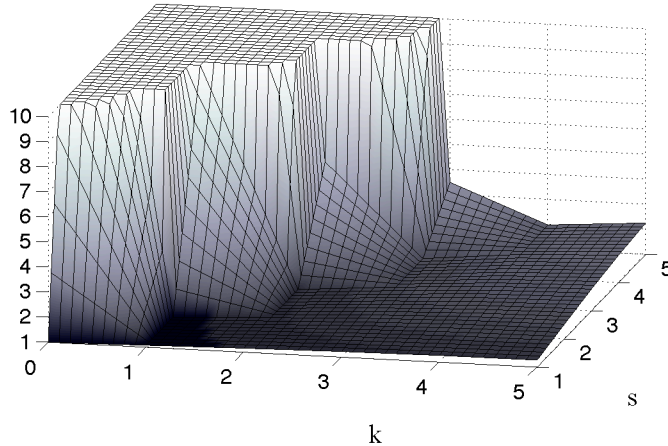
By analyzing trends in the optimality surface, one can determine two traits: *accuracy* and *robustness*. Accuracy is a measure of how close the optimality surface is to one at a point. Hence, accuracy is an indicator of how close to optimal a spline space is for a given smooth function space. Robustness, on the other hand, is a measure of how far one can drift on the optimality surface from an optimal (or near optimal) point without losing much accuracy. This definition will become clearer as we discuss our numerical results.

#### 5.3.1 $L^2$ optimality surfaces: Sobolev spaces

We first compute optimality surfaces for the case of approximating Sobolev spaces in the  $L^2$  norm. The reader may ask why we are using approximations in the  $L^2$  norm as opposed to the  $H^1$  norm or semi-norm as is standard in finite elements. The reasoning for this choice is simple: when measuring errors in the  $H^1$  semi-norm, we are simply measuring the *error of the derivative* in the  $L^2$  norm. Consequently, by measuring how well piecewise constants approximate  $H^1(0, 1)$  in the  $L^2$  norm, we are in fact also measuring how well piecewise linears approximate the Sobolev space  $H^2(0, 1)$  in the  $H^1$  semi-norm. Since the derivatives of spline functions of maximal continuity are again spline functions of maximal continuity, a similar relationship holds for higher-order splines.

Before discussing our numerical results, let us recall the accuracy result stated in Example 4.2: there exist spline spaces of order  $s - 1$  which are optimal for the  $n$ -width  $d_n(\tilde{B}^s(0, 1); L^2(0, 1))$ . Hence, we expect that splines of order  $s - 1$  are nearly optimal in approximating functions in  $H^s$ . As the order of our splines is increased above  $s - 1$ , we might expect our approximation properties to deteriorate as we are incorporating functions of higher regularity than the space we are trying to approximate. However, we shall see that there is little or no deterioration. As the order of our splines is decreased below  $s - 1$ , we expect our approximation properties to deteriorate rapidly.

We have computed the optimality ratio  $\Lambda(B^s(0, 1), K(n, k, 0, 1); L^2(0, 1))$  for the cases of  $n = 10, 20$ , and  $30$  and reported the results in Figures 5, 6, and 7 respectively. For purposes of ease of visualization, we have capped off the optimality surface plots at the value  $\Lambda = 10$ . We immediately see that as expected, uniform spline spaces of order  $s - 1$  are nearly optimal in approximating functions in  $H^s$ . This is the *accuracy* result we were looking for, and we have colored the corresponding cells in Figures 5, 6, and 7 to highlight this result. However, we also have a strong *robustness* result: uniform spline spaces of order  $k > s - 1$  are nearly optimal in approximating  $H^s$  as well. In fact, we see little increase in the optimality ratio as the polynomial order  $k$  is increased, and this increase becomes smaller as the number of degrees of freedom is increased. This indicates that there is very little penalty for choosing too smooth a spline space in solving a partial differential equation with the finite element method. Finally, as expected, we see that if we choose splines with lower order than optimal,



	$k = 0$	$k = 1$	$k = 2$	$k = 3$	$k = 4$	$k = 5$
$s = 5$	2.8e+05	4.5e+03	1.0e+02	3.5e+00	2.0e+00	2.3e+00
$s = 4$	1.4e+04	2.3e+02	5.2e+00	1.6e+00	1.9e+00	2.1e+00
$s = 3$	6.3e+02	1.0e+01	1.3e+00	1.6e+00	1.8e+00	1.9e+00
$s = 2$	2.5e+01	1.1e+00	1.3e+00	1.4e+00	1.5e+00	1.6e+00
$s = 1$	1.0e+00	1.1e+00	1.2e+00	1.2e+00	1.3e+00	1.3e+00

Figure 5:  $L^2$  optimality surface and a table of  $L^2$  optimality ratios  $\Lambda$  for the  $k$ -method in approximating the  $H^s$  unit ball with 10 degrees of freedom

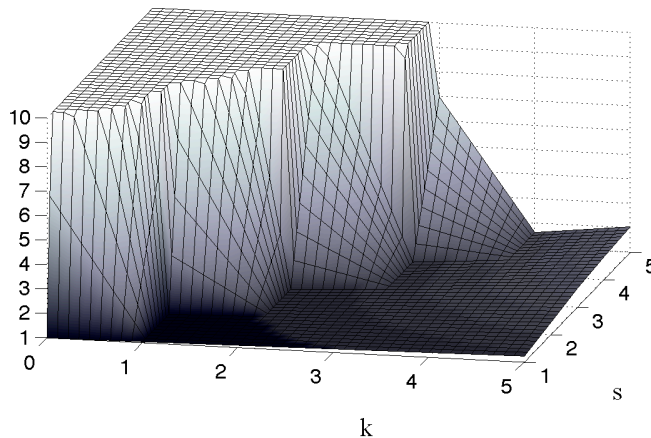
our results rapidly deteriorate.

Comparing our results for  $n = 10, 20,$  and  $30$ , we find another powerful result. Provided that  $k \geq s - 1$ , we find that the optimality ratio  $\Lambda(B^s(0, 1), K(n, k, 0, 1); L^2(0, 1))$  decreases with increasing  $n$ . This seems to indicate that in the limit as  $n \rightarrow \infty$ , uniform spline spaces of sufficient order are in fact optimal spaces for approximating Sobolev spaces. This result is not entirely surprising. Through the course of numerically analyzing the optimal knot locations as indicated in Example 4.2, we found that the knots become more equispaced as the number of degrees of freedom was increased. Hence, we make the following conjecture regarding the asymptotic accuracy of higher-order  $k$ -methods.

**Conjecture 5.1. (Optimality of Splines in the Limit)** *For fixed non-negative integers  $k, s$  satisfying  $k \geq s - 1$ , the following relationship holds:*

$$\lim_{n \rightarrow \infty} \Lambda(B^s(0, 1), K(n, k, 0, 1); L^2(0, 1)) = 1. \quad (102)$$

We feel a further analysis of the conjecture warrants merit, and such an analysis might prove to be instrumental to advancing spline-based finite element approximation theory.



	$k = 0$	$k = 1$	$k = 2$	$k = 3$	$k = 4$	$k = 5$
$s = 5$	8.2e+06	5.8e+04	5.4e+02	7.0e+00	1.6e+00	2.0e+00
$s = 4$	1.6e+05	1.1e+03	1.1e+01	1.3e+00	1.6e+00	1.9e+00
$s = 3$	3.0e+03	2.1e+01	1.1e+00	1.3e+00	1.6e+00	1.8e+00
$s = 2$	5.2e+01	1.0e+00	1.1e+00	1.3e+00	1.4e+00	1.5e+00
$s = 1$	1.0e+00	1.0e+00	1.1e+00	1.1e+00	1.2e+00	1.2e+00

Figure 6:  $L^2$  optimality surface and a table of  $L^2$  optimality ratios  $\Lambda$  for the  $k$ -method in approximating the  $H^s$  unit ball with 20 degrees of freedom

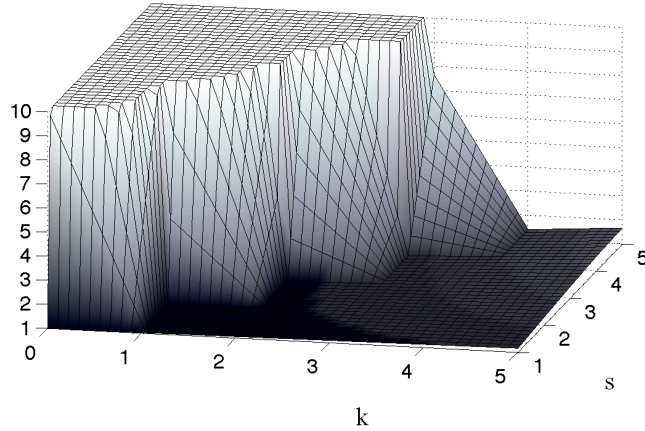
### 5.3.2 $L^2$ optimality surfaces: periodic Sobolev spaces

We continue this subsection by computing optimality surfaces for the case of approximating periodic Sobolev spaces in the  $L^2$  norm. We consider separately the cases of even and odd numbers of degrees of freedom. The reason for this will become clear in the sequel.

*Case 1: Even number of degrees of freedom*

Example 4.3 demonstrated that for  $s \geq 2$  and for even numbers of degrees of freedom, periodic splines of order  $s - 1$  were optimal in approximating  $\tilde{B}_{per}^s(0, 2\pi)$  in the  $L^2$  norm. Thus, the main question for periodic spline spaces of even dimension is *robustness*: what happens to our approximation properties as the order of our splines is increased? The previous results in regards to standard Sobolev spaces suggest that increasing our polynomial order has little effect on our approximability, and our numerical results here hint at an even stronger result for periodic splines.

As before, we have computed the optimality ratio  $\Lambda(B_{per}^s(0, 2\pi), K_{per}(n, k, 0, 2\pi); L^2(0, 2\pi))$  for the cases of  $n = 10, 20,$  and  $30$  and reported the results in Figures 8, 9, and 10. By analyzing the figures, we immediately see the remarkable accuracy result: for  $k \geq s - 1$  and  $n$  even, uniform periodic splines of order  $k$  are optimal in approximating the unit ball  $B_{per}^s(0, 2\pi)$  of  $H_{per}^s(0, 2\pi)$ . Analogous to the Sobolev case analyzed earlier, we have colored the corresponding cells in Figures 8, 9, and 10 to highlight this result.



	$k = 0$	$k = 1$	$k = 2$	$k = 3$	$k = 4$	$k = 5$
$s = 5$	5.0e+07	2.3e+05	1.3e+03	7.6e+00	1.4e+00	1.7e+00
$s = 4$	6.0e+05	2.8e+03	1.6e+01	1.2e+00	1.4e+00	1.6e+00
$s = 3$	7.0e+03	3.2e+01	1.1e+00	1.2e+00	1.3e+00	1.5e+00
$s = 2$	7.9e+01	1.0e+00	1.1e+00	1.2e+00	1.3e+00	1.3e+00
$s = 1$	1.0e+00	1.0e+00	1.1e+00	1.1e+00	1.1e+00	1.2e+00

Figure 7:  $L^2$  optimality surface and a table of  $L^2$  optimality ratios  $\Lambda$  for the  $k$ -method in approximating the  $H^s$  unit ball with 30 degrees of freedom

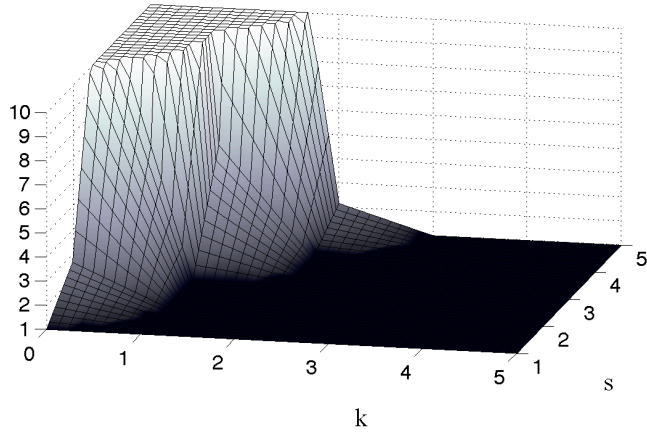
**Conjecture 5.2. (Optimality of Periodic Splines)** For non-negative integers  $k, s$  satisfying  $k \geq s - 1$ , the relationship

$$\Lambda(B_{per}^s(0, 1), K(n, k, 0, 1); L^2(0, 1)) = 1 \quad (103)$$

holds for all even  $n \in \mathbb{N}$ .

Conjecture 5.2 suggests that the periodic  $k$ -method has essentially identical approximation powers as the Fourier spectral method. However, unlike the spectral method, the  $k$ -method employs functions with compact support and hence results in sparse systems, even for the case of nonlinear problems. As such systems lend themselves well to robust, parallel solvers, the periodic  $k$ -method, with its spectral accuracy properties, is an accurate and efficient method for a number of application areas (as we have in fact already seen in turbulence [1, 8]).

Analyzing Figures 8, 9, and 10 more closely, we see that for the most part, spline spaces with lower than optimal polynomial order and hence lower continuity have poor approximation properties. However, we do witness some pre-asymptotic behavior in the associated optimality surfaces. For example, for  $n = 10$ , we find that spline functions of order 1 are optimal for approximating  $H^3(0, 2\pi)$ , while for  $n = 10$  and 20, spline functions of order 2 are optimal for approximating  $H^4(0, 2\pi)$ . We have colored the corresponding cells in Figures



	$k = 0$	$k = 1$	$k = 2$	$k = 3$	$k = 4$	$k = 5$
$s = 5$	3.3e+02	2.7e+01	2.1e+00	1.0e+00	1.0e+00	1.0e+00
$s = 4$	6.7e+01	5.5e+00	1.0e+00	1.0e+00	1.0e+00	1.0e+00
$s = 3$	1.3e+01	1.0e+00	1.0e+00	1.0e+00	1.0e+00	1.0e+00
$s = 2$	2.7e+00	1.0e+00	1.0e+00	1.0e+00	1.0e+00	1.0e+00
$s = 1$	1.0e+00	1.0e+00	1.0e+00	1.0e+00	1.0e+00	1.0e+00

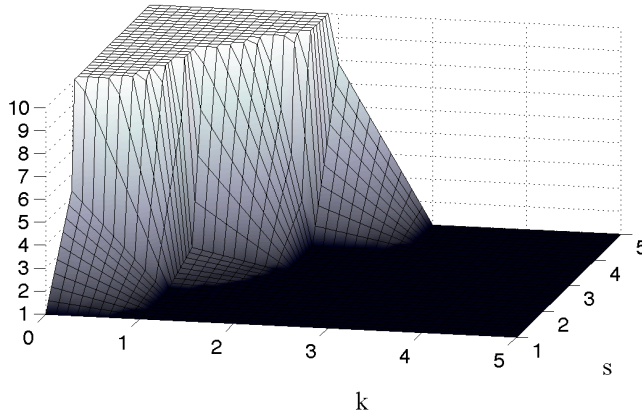
Figure 8:  $L^2$  optimality surface and a table of  $L^2$  optimality ratios  $\Lambda$  for the  $k$ -method in approximating the  $H_{per}^s$  unit ball with 10 degrees of freedom

8, 9, and 10 a lighter shade of gray to highlight this interesting result. This pre-asymptotic behavior suggests possible advantages to employing lower-order spline spaces for small numbers of degrees of freedom, but a further analysis should be conducted before any clear conclusions are made.

*Case 2: Odd number of degrees of freedom*

The situation changes when periodic spaces of odd dimension are employed. No theoretical results concerning the optimality of these spaces exist. Nonetheless, one would expect a similar behavior to that of classical Sobolev spaces. That is, for odd numbers of degrees of freedom, one expects periodic splines of order  $s - 1$  to be near optimal in approximating  $H_{per}^s(0, 2\pi)$  and that increasing the polynomial order slightly decreases the accuracy. Numerical results, however, paint a nicer picture.

In Figure 11, we have plotted the optimality ratio  $\Lambda(B_{per}^s(0, 2\pi), K_{per}(n, k, 0, 2\pi); L^2(0, 2\pi))$  for  $n = 15$ . From this picture, we confirm that periodic spline spaces of order  $s - 1$  and odd dimension are nearly optimal in approximating  $H_{per}^s(0, 2\pi)$ , but increasing the polynomial order, contrary to what we expected, actually *improves* our accuracy. This result further validates what we have already seen: the  $k$ -method is an *accurate and robust* solution methodology. Increasing the order and continuity of spline finite elements allows one to capture smoother functions more accurately without hampering approximability of rougher



	$k = 0$	$k = 1$	$k = 2$	$k = 3$	$k = 4$	$k = 5$
$s = 5$	5.3e+03	1.9e+02	7.8e+00	1.0e+00	1.0e+00	1.0e+00
$s = 4$	5.3e+02	1.9e+01	1.0e+00	1.0e+00	1.0e+00	1.0e+00
$s = 3$	5.3e+01	1.9e+00	1.0e+00	1.0e+00	1.0e+00	1.0e+00
$s = 2$	5.3e+00	1.0e+00	1.0e+00	1.0e+00	1.0e+00	1.0e+00
$s = 1$	1.0e+00	1.0e+00	1.0e+00	1.0e+00	1.0e+00	1.0e+00

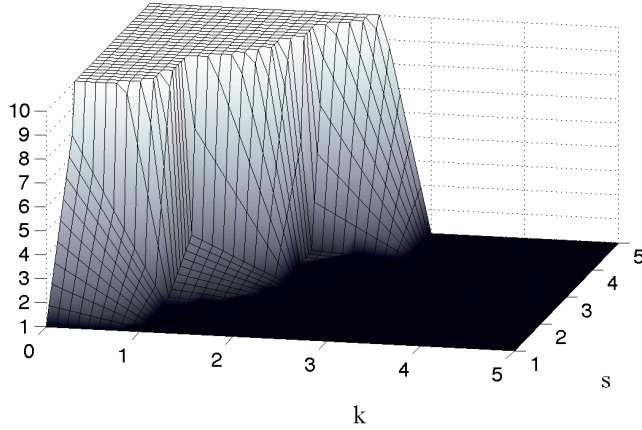
Figure 9:  $L^2$  optimality surface and a table of  $L^2$  optimality ratios  $\Lambda$  for the  $k$ -method in approximating the  $H_{per}^s$  unit ball with 20 degrees of freedom

functions (and in this case, it improves accuracy all around).

### 5.3.3 $L^2$ optimality surfaces: Weighted Sobolev spaces

We next compute optimality surfaces for the case of approximating weighted Sobolev spaces in the  $L^2$  norm. The spaces we consider here are the Legendre-weighted Sobolev spaces  $V_s^s(-1, 1)$ . In Example 4.4, we showed that polynomial spaces are optimal in approximating such spaces, so we are interested in the accuracy of lower-order splines. Such results will indicate how well the  $k$ -method can approximate singularities in finite element solutions. As no mathematical theory has yet been done in the context of using the  $k$ -method for approximating singular solutions, the results here are new and present possible research opportunities.

We have computed the optimality ratio  $\Lambda(B_w^{s,s}(-1, 1), K(n, k, -1, 1); L^2(-1, 1))$  for the cases of  $n = 10, 20,$  and  $30$  and reported the results in Figures 12, 13, and 14. As expected, for each  $s$ , the ratios decrease as the order  $k$  of the splines is increased, and for fixed  $k$  and  $s$ , the ratio increases as the number of splines  $n$  is increased. What is promising is the fact that for each  $s$ , the ratios seem to decrease in a rapid fashion. As such, fairly low-order splines can exhibit good behavior in approximating non-smooth functions. Analyzing the figures, we find a good rule of thumb is to employ splines of at least order  $s$  when approximating the space  $V_s^s(-1, 1)$ . We find that increasing the order beyond this point does little in terms of improving accuracy while decreasing the order beyond this limit tends to drastically degrade



	$k = 0$	$k = 1$	$k = 2$	$k = 3$	$k = 4$	$k = 5$
$s = 5$	2.7e+04	6.3e+02	1.8e+01	1.0e+00	1.0e+00	1.0e+00
$s = 4$	1.8e+03	4.2e+01	1.2e+00	1.0e+00	1.0e+00	1.0e+00
$s = 3$	1.2e+02	2.8e+00	1.0e+00	1.0e+00	1.0e+00	1.0e+00
$s = 2$	7.9e+00	1.0e+00	1.0e+00	1.0e+00	1.0e+00	1.0e+00
$s = 1$	1.0e+00	1.0e+00	1.0e+00	1.0e+00	1.0e+00	1.0e+00

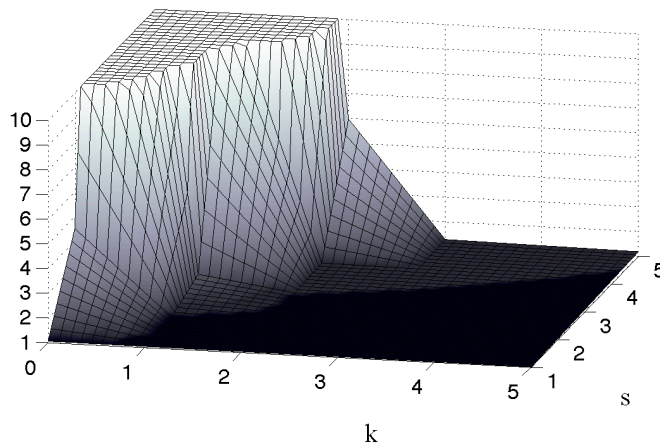
Figure 10:  $L^2$  optimality surface and a table of  $L^2$  optimality ratios  $\Lambda$  for the  $k$ -method in approximating the  $H_{per}^s$  unit ball with 30 degrees of freedom

accuracy. Of course, a more rigorous analysis of this case would provide much more intuition as to choosing an appropriate measure as to which splines to employ in different situations.

### 5.3.4 $H^1$ optimality surfaces: Sobolev spaces

We finish this subsection by computing optimality surfaces for the case of approximating Sobolev spaces in the  $H^1$  norm. We feel this is an important case as many *a priori* finite element error estimates are in terms of the  $H^1$  norm of the solution as opposed to the  $L^2$  norm of the derivative of the solution. However, as most theoretical results for  $n$ -widths involve compact operators of  $L^2$  (such as Theorems 4.1 through Theorem 4.4), not much work has been done in the context of analytically finding optimal spaces for the  $H^1$  counterpart. On the other hand, Theorems 4.5 and 4.6 may still be employed in order to determine  $n$ -widths and sup-infs computationally.

We have computed the optimality ratio  $\Lambda(B^s(0, 1), K(n, k, 0, 1); H^1(0, 1))$  for the cases of  $n = 10, 20,$  and  $30$  and reported the results in Figures 15, 16, and 17. We find that the optimality surfaces share the same characteristics as those corresponding to the  $L^2$  norm, namely that splines of order  $k \geq s - 1$  are nearly optimal in approximating functions in  $H^s$ . Indeed, preliminary numerical experiments reveal that these same characteristics hold for higher-order Sobolev norms as well. We thus present the following conjecture as a generalization of Conjecture 5.1.



	$k = 0$	$k = 1$	$k = 2$	$k = 3$	$k = 4$	$k = 5$
$s = 5$	1.6e+03	9.0e+01	6.0e+00	1.3e+00	1.2e+00	1.2e+00
$s = 4$	2.2e+02	1.2e+01	1.3e+00	1.2e+00	1.2e+00	1.1e+00
$s = 3$	3.1e+01	1.7e+00	1.2e+00	1.1e+00	1.1e+00	1.1e+00
$s = 2$	4.5e+00	1.1e+00	1.1e+00	1.1e+00	1.1e+00	1.1e+00
$s = 1$	1.1e+00	1.1e+00	1.0e+00	1.0e+00	1.0e+00	1.0e+00

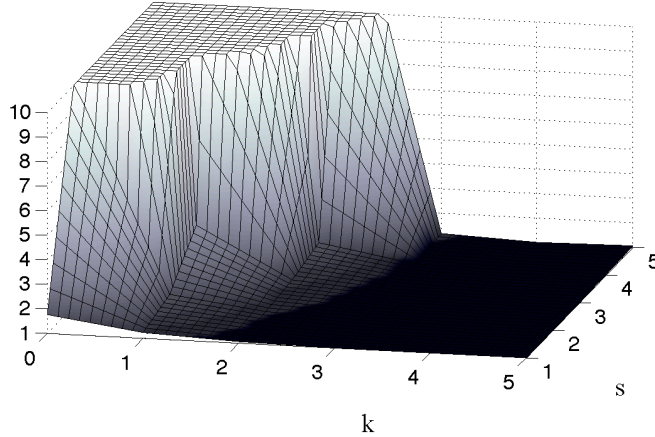
Figure 11:  $L^2$  optimality surface and a table of  $L^2$  optimality ratios  $\Lambda$  for the  $k$ -method in approximating the  $H_{per}^s$  unit ball with 15 degrees of freedom

**Conjecture 5.3. (Optimality of Splines in the Limit for General Sobolev Norms)**  
For fixed non-negative integers  $r, k, s$  satisfying  $k \geq s-1$  and  $s > r$ , the following relationship holds:

$$\lim_{n \rightarrow \infty} \Lambda(B^s(0, 1), K(n, k, 0, 1); H^r(0, 1)) = 1. \quad (104)$$

### 5.3.5 Discussion

The preceding results indicate that the  $k$ -method is an accurate and robust method of approximating a large class of functions. In the context of Sobolev and periodic Sobolev spaces, we witnessed that spline spaces are nearly optimal and that increasing the order of a spline space improved our approximability of smooth functions without reducing our accuracy in approximating rough ones. For weighted Sobolev spaces, we saw that increasing the order of a spline space in fact improved our accuracy in a rapid fashion. These results validate what we have already seen in numerical simulations: higher-order higher-continuous spline functions are an accurate and robust candidate for finite element approximation. Finally, we note that the three conjectures stated the convergence behavior of the  $k$ -method as  $n \rightarrow \infty$  with  $k$  and  $s$  fixed. We feel it is also important to study the behavior of the method given a specific relationship between the number of degrees of freedom and the degree of the spline functions.



	$k = 0$	$k = 1$	$k = 2$	$k = 3$	$k = 4$	$k = 5$
$s = 5$	1.0e+04	3.2e+02	1.6e+01	1.1e+00	1.0e+00	1.0e+00
$s = 4$	1.0e+03	3.3e+01	1.7e+00	1.1e+00	1.0e+00	1.0e+00
$s = 3$	1.0e+02	3.4e+00	1.3e+00	1.0e+00	1.0e+00	1.0e+00
$s = 2$	1.0e+01	1.7e+00	1.2e+00	1.0e+00	1.0e+00	1.0e+00
$s = 1$	1.8e+00	1.2e+00	1.1e+00	1.0e+00	1.0e+00	1.0e+00

Figure 12:  $L^2$  optimality surface and a table of  $L^2$  optimality ratios  $\Lambda$  for the  $k$ -method in approximating the  $V_s^s$  unit ball with 10 degrees of freedom

## 5.4 Comparison study of the classical finite element and $k$ -methods using optimality ratios

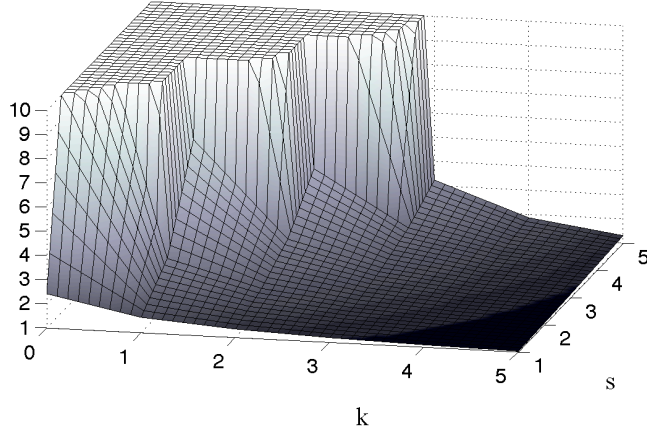
In this subsection, we conduct a comparison study of the classical finite element and  $k$ -methods using optimality ratios. As motivation, we know that for sufficiently smooth functions, the following relation holds:

If  $\pi_n$  denotes the  $L^2$ -projector onto an  $n$ -dimensional spline space of order  $s-1$  with uniformly spaced knots, then

$$\|u - \pi_n u\|_{L^2(0,1)} \leq C n^{-s} \|u\|_{H^s(0,1)} \quad (105)$$

where  $C$  depends only on the order and continuity of the spline functions [9].

Thus, we know the classical finite element and  $k$ -methods share the same asymptotic approximation behaviors. The questions are: what is  $C$  for each of the methods, and how do they compare? These questions can be answered through the use of the *comparison ratio* defined in Equation (20). Note that in this analysis, we compare the methods only in terms of accuracy as defined by the optimality ratio. We do not include factors such as computational costs in our comparison metric, but we do feel such factors should be included when one decides which method to utilize.



	$k = 0$	$k = 1$	$k = 2$	$k = 3$	$k = 4$	$k = 5$
$s = 5$	1.3e+05	2.7e+03	9.2e+01	3.2e+00	1.8e+00	1.3e+00
$s = 4$	6.7e+03	1.4e+02	4.6e+00	2.4e+00	1.6e+00	1.2e+00
$s = 3$	3.3e+02	6.7e+00	2.8e+00	1.8e+00	1.4e+00	1.2e+00
$s = 2$	1.6e+01	3.0e+00	1.9e+00	1.5e+00	1.2e+00	1.1e+00
$s = 1$	2.4e+00	1.6e+00	1.4e+00	1.2e+00	1.1e+00	1.0e+00

Figure 13:  $L^2$  optimality surface and a table of  $L^2$  optimality ratios  $\Lambda$  for the  $k$ -method in approximating the  $V_s^s$  unit ball with 20 degrees of freedom

We have computed the two optimality ratio pairs

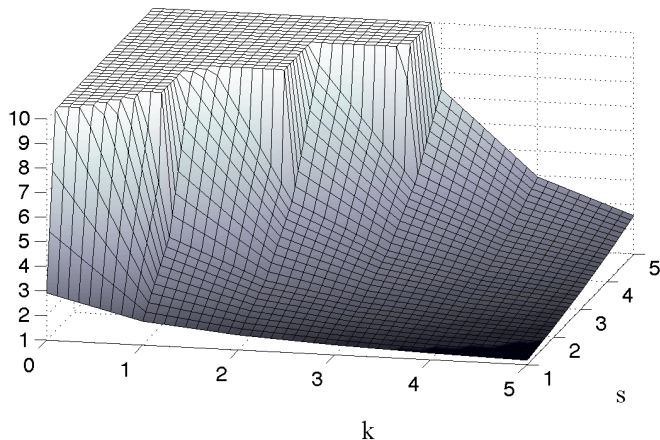
$$\left\{ \Lambda(B^s(-1, 1), P(n, s - 1, 0, 1); L^2(0, 1)), \Lambda(B^s(-1, 1), K(n, s - 1, 0, 1); L^2(0, 1)) \right\}, \quad (106)$$

$$\left\{ \Lambda(B^s(-1, 1), P(n, s - 1, 0, 1); H^1(0, 1)), \Lambda(B^s(-1, 1), K(n, s - 1, 0, 1); H^1(0, 1)) \right\} \quad (107)$$

as functions of  $n$  for  $s = 2, 3$ , and  $4$  and plotted the results in Figures 18 and 19 respectively. Note that the classical finite element method is labeled as  $C^0$  FEM in both figures.

The two figures show that the  $k$ -method outperforms the classical finite element method for all three polynomial orders on a per degree-of-freedom basis. Further, we see that the difference between the performance of the  $k$ -method and the classical finite element method grows as a function of the polynomial order. What is more astonishing is that while the  $k$ -method optimality ratio deteriorates as the number of degrees of freedom is increased, the classical finite element method optimality ratio increases. We feel that a thorough understanding of how large the optimality ratio becomes for the classical finite element method for assorted polynomial orders would be of much interest to the finite element community and may highlight some of the similarities and differences between the classical finite element and  $k$ -methods.

Another observation we make is that the  $H^1$  optimality ratios associated with the  $k$ -method tend to be smaller than the corresponding  $L^2$  optimality ratios, while the  $H^1$  ratios associated with the classical finite element method tend to be larger than the associated



	$k = 0$	$k = 1$	$k = 2$	$k = 3$	$k = 4$	$k = 5$
$s = 5$	6.7e+05	1.0e+04	2.8e+02	7.3e+00	3.9e+00	2.6e+00
$s = 4$	2.2e+04	3.4e+02	9.2e+00	4.6e+00	2.9e+00	2.1e+00
$s = 3$	7.3e+02	1.1e+01	4.8e+00	3.0e+00	2.1e+00	1.7e+00
$s = 2$	2.4e+01	4.3e+00	2.7e+00	2.0e+00	1.6e+00	1.4e+00
$s = 1$	2.9e+00	2.0e+00	1.6e+00	1.4e+00	1.3e+00	1.2e+00

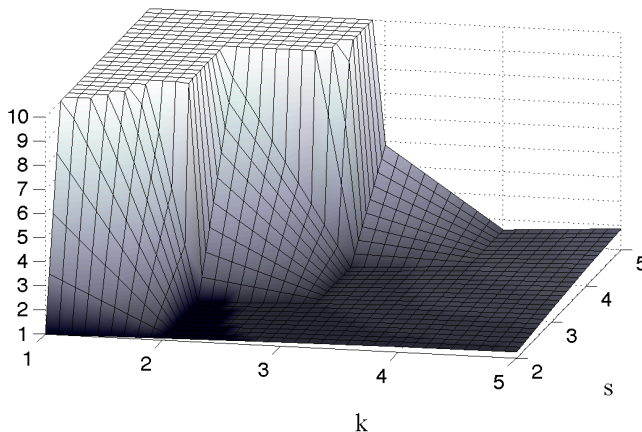
Figure 14:  $L^2$  optimality surface and a table of  $L^2$  optimality ratios  $\Lambda$  for the  $k$ -method in approximating the  $V_s^s$  unit ball with 30 degrees of freedom

$L^2$  ratios. This seems to suggest once again that  $k$ -methods are a promising candidate for approximating solutions to second-order elliptic boundary value problems as a natural norm for such problems is the  $H^1$  norm.

An alternative view by which we can compare two spaces is by analyzing the percent error by which their sup-infs are from the  $n$ -width. We refer to this percentage as the *optimality error*, and it is defined by

$$\mathcal{E}_n(A, X_n; X) = 100 \left( \frac{E(A, X_n; X) - d_n(A; X)}{d_n(A; X)} \right) \% = 100 (\Lambda(A, X_n; X) - 1) \%. \quad (108)$$

Returning to Figures 18 and 19, we find that the optimality error is very small for the  $k$ -method and quite large for the classical finite element method. Further, the optimality error grows in terms of increasing number of degrees of freedom for the classical finite element method while it diminishes for the  $k$ -method. For the case of quadratics approximating the  $H^3$  unit ball in terms of the  $L^2$  norm, we find that the optimality error grows to 70% for the classical finite element method while the error reduces to 7% for the  $k$ -method as the number of degrees of freedom approaches 43. The effect is more pronounced for higher polynomial orders and higher-order Sobolev norms. For the case of quartics approximating the  $H^5$  unit ball in terms of the  $H^1$  norm, the error grows to 488% for the classical finite element method while the error reduces to 13% for the  $k$ -method as the number of degrees of freedom approaches 49.



	$k = 1$	$k = 2$	$k = 3$	$k = 4$	$k = 5$
$s = 5$	9.6e+03	1.7e+02	4.8e+00	1.6e+00	1.9e+00
$s = 4$	4.9e+02	8.9e+00	1.3e+00	1.6e+00	1.7e+00
$s = 3$	2.2e+01	1.1e+00	1.3e+00	1.4e+00	1.5e+00
$s = 2$	1.0e+00	1.1e+00	1.2e+00	1.2e+00	1.3e+00

Figure 15:  $H^1$  optimality surface and a table of  $H^1$  optimality ratios  $\Lambda$  for the  $k$ -method in approximating the  $H^s$  unit ball with 10 degrees of freedom

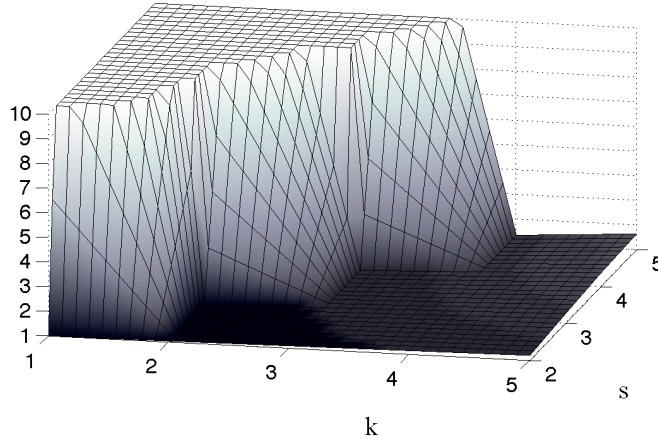
## 5.5 Robustness of polynomial approximation

We finish with a short analysis of the robustness properties of polynomial approximation. In this study, we consider approximating functions with global polynomials as opposed to piecewise polynomials as before. Such methods are referred to as *spectral methods*, and these may be thought of as the intersection of the classical finite element and  $k$ -methods. We know that high-order polynomials are accurate approximants for smooth functions, but we are now interested in how accurate high-order polynomials are in approximating rough functions on a per degree-of-freedom basis.

In Figure 20, we have plotted the optimality ratios  $\Lambda(B^s(0, 1), \mathcal{P}(p + 1, 0, 1); L^2(0, 1))$  for  $p = 0$  through  $p = 10$  and  $s = 1, 2, 3$ . We see immediately that for each of these cases, the optimality ratio is bounded above by 2, and hence high-order polynomials are nearly optimal approximants. Further, seemingly counter-intuitively, higher-order polynomials are more accurate in terms of the optimality ratio for spaces of lower smoothness than spaces of moderate smoothness.

## 6 Conclusions

In this paper, we have conducted a mathematical study of the  $k$ -method utilizing results in approximation theory. Theoretical results indicate that for many function spaces, higher-order splines with maximal continuity are optimal approximants with respect to the number of degrees of freedom, and numerical studies have validated and improved these results.



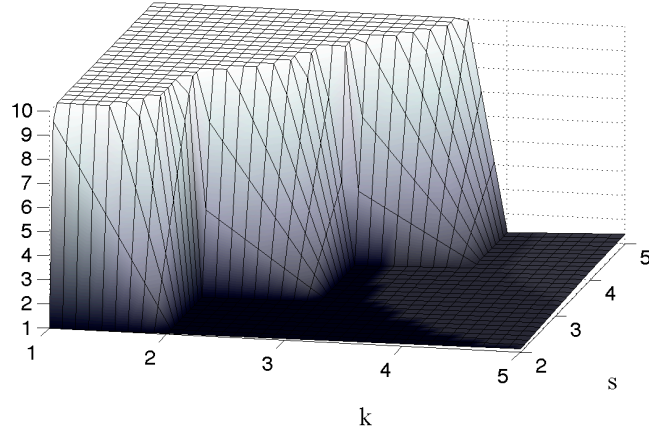
	$k = 1$	$k = 2$	$k = 3$	$k = 4$	$k = 5$
$s = 5$	1.3e+05	1.0e+03	2.0e+01	1.4e+00	1.6e+00
$s = 4$	2.7e+03	2.0e+01	1.2e+00	1.4e+00	1.6e+00
$s = 3$	5.0e+01	1.0e+00	1.2e+00	1.3e+00	1.4e+00
$s = 2$	1.0e+00	1.0e+00	1.1e+00	1.2e+00	1.2e+00

Figure 16:  $H^1$  optimality surface and a table of  $H^1$  optimality ratios  $\Lambda$  for the  $k$ -method in approximating the  $H^s$  unit ball with 20 degrees of freedom

A numerical comparison of the classical finite element and  $k$ -methods revealed that the  $k$ -method has better approximation properties than the classical finite element method on a per degree-of-freedom basis, further suggesting that the  $k$ -method is an accurate and robust scheme for approximating solutions to partial differential equations. These results are consistent with observations made previously based on discrete Fourier analysis and the numerical solutions of boundary value problems [1, 8, 15, 16, 22]. It should be noted, however, that these comparisons did not take into account other factors such as computation time. In the future, we hope to extend these results to the multi-dimensional and rational setting utilizing the theoretical and computational framework we have developed here. In addition, we hope to analyze the local approximation behavior around singularities and develop *a posteriori* error estimation procedures for the  $k$ -method.

## Acknowledgements

J.A. Evans was partially supported by the Department of Energy Computational Science Graduate Fellowship, provided under grant number DE-FG02-97ER25308. Y. Bazilevs was partially supported by the J.T. Oden ICES Postdoctoral Fellowship at the Institute for Computational Engineering and Sciences (ICES). Y. Bazilevs and T.J.R. Hughes were partially supported by the Office of Naval Research under Construct No. N00014-03-0263. This support is gratefully acknowledged.



	$k = 1$	$k = 2$	$k = 3$	$k = 4$	$k = 5$
$s = 5$	5.4e+05	2.6e+03	2.7e+01	1.2e+00	1.4e+00
$s = 4$	6.6e+03	3.2e+01	1.1e+00	1.2e+00	1.4e+00
$s = 3$	7.7e+01	1.0e+00	1.1e+00	1.2e+00	1.3e+00
$s = 2$	1.0e+00	1.0e+00	1.1e+00	1.1e+00	1.1e+00

Figure 17:  $H^1$  optimality surface and a table of  $H^1$  optimality ratios  $\Lambda$  for the  $k$ -method in approximating the  $H^s$  unit ball with 30 degrees of freedom

## References

- [1] Akkerman, I., Bazilevs, Y., Calo, V.M., Hughes, T.J.R., Hulshoff, S.: The role of continuity in residual-based variational multiscale modeling of turbulence. *Computational Mechanics* **41**, 371–378 (2008)
- [2] Aubin, J.P.: *Approximation of Elliptic Boundary Value Problems*. Wiley (1972)
- [3] Babuška, I.: Finite element method for domains with corners. *Computing* **6**, 264–273 (1970)
- [4] Babuška, I., Banerjee, U., Osborn, J.E.: On principles for the selection of shape functions for the Generalized Finite Element Method. *Computer Methods in Applied Mechanics and Engineering* **191**, 5595–5629 (2002)
- [5] Babuška, I., Osborn, J.: Eigenvalue Problems. In: P.G. Ciarlet, J.L. Lions (eds.) *Handbook of Numerical Analysis, vol. II, Finite Element Methods (Part I)*, pp. 641–787. North-Holland (1991)
- [6] Babuška, I., Suri, M.: The  $h - p$  version of the finite element method with quasiuniform meshes. *Modélisation Mathématique et Analyse Numérique- RAIRO* **21**, 199–238 (1987)
- [7] Babuška, I., Suri, M.: The optimal convergence rate of the  $p$ -version of the finite element method. *SIAM Journal of Numerical Analysis* **24**, 750–776 (1987)

- [8] Bazilevs, Y., Calo, V.M., Cottrell, J.A., Hughes, T.J.R., Reali, A., Scovazzi, G.: Variational multiscale residual-based turbulence modeling for large eddy simulation of incompressible flows. *Computer Methods in Applied Mechanics and Engineering* **197**, 173–201 (2007)
- [9] Bazilevs, Y., da Veiga, L.B., Cottrell, J.A., Hughes, T.J.R., Sangalli, G.: Isogeometric analysis: Approximation, stability and error estimates for  $h$ -refined meshes. *Mathematical Models and Methods in Applied Sciences* **16**, 1–60 (2006)
- [10] Bernardi, C., Maday, Y.: Polynomial approximation of some singular functions. *Applicable Analysis* **42**, 1–32 (1991)
- [11] de Boor, C.R.: On calculating with B-splines. *Journal of Approximation Theory* **6**, 45–99, 50–62 (1972)
- [12] de Boor, C.R.: *A Practical Guide to Splines*. Springer-Verlag (1978)
- [13] Ciarlet, P.G.: *The Finite Element Method for Elliptic Problems*. SIAM: Society for Industrial and Applied Mathematics (2002)
- [14] Cohen, E., Riesenfeld, R.F., Elber, G.: *Geometric Modeling with Splines*. A K Peters (2001)
- [15] Cottrell, J.A., Hughes, T.J.R., Reali, A.: Studies of refinement and continuity in isogeometric structural analysis. *Computer Methods in Applied Mechanics and Engineering* **196**, 4160–4183 (2006)
- [16] Cottrell, J.A., Reali, A., Bazilevs, Y., Hughes, T.J.R.: Isogeometric analysis of structural vibrations. *Computer Methods in Applied Mechanics and Engineering* **195**, 5257–5297 (2006)
- [17] Gerdes, K., Demkowicz, L.: Solution of 3D-Laplace and Helmholtz equations in exterior domains using  $hp$ -infinite elements. *Computer Methods in Applied Mechanics and Engineering* **137**, 239–273 (1996)
- [18] Golub, G.H., Ye, Q.: An inverse free preconditioned Krylov subspace method for symmetric generalized eigenvalue problems. *SIAM Journal on Scientific Computing* **24**, 312–334 (2002)
- [19] Gurka, P., Opic, B.: Continuous and compact imbeddings of weighted Sobolev spaces I. *Czechoslovak Mathematical Journal* **38**, 730–744 (1988)
- [20] Höllig, K.: *Finite Element Methods with B-splines*. Society for Industrial and Applied Mathematics (2003)
- [21] Hughes, T.J.R., Cottrell, J.A., Bazilevs, Y.: Isogeometric analysis: CAD, finite elements, NURBS, exact geometry, and mesh refinement. *Computer Methods in Applied Mechanics and Engineering* **194**, 4135–4195 (2005)

- [22] Hughes, T.J.R., Reali, A., Sangalli, G.: Duality and unified analysis of discrete approximations in structural dynamics and wave propagation: Comparison of  $p$ -method finite elements with  $k$ -method NURBS. *Computer Methods in Applied Mechanics and Engineering* (2008). In press.
- [23] Kolmogorov, A.: Über die beste annäherung van funktionen einer gegebenen funktionsklasse. *Annals of Mathematics* **37**, 107–110 (1936)
- [24] Melkman, A.A., Micchelli, C.A.: Spline spaces are optimal for  $L^2$   $n$ -widths. *Illinois Journal of Mathematics* **22**, 541–564 (1978)
- [25] Piegl, L., Tiller, W.: *The NURBS Book*, 2nd Edition. Springer-Verlag (1997)
- [26] Pinkus, A.:  *$n$ -Widths in Approximation Theory*. Springer-Verlag, Berlin (1980)
- [27] Rogers, D.F.: *An Introduction to NURBS With Historical Perspective*. Academic Press (2001)
- [28] Schoenberg, I.J.: Contributions to the problem of approximation of equidistant data by analytic functions. *Quarterly of Applied Mathematics* **4**, 45–99, 112–141 (1946)
- [29] Schumaker, L.: *Spline Functions: Basic Theory*. Wiley (1981)
- [30] Schwab, C., Suri, M.: The optimal  $p$ -version approximation of singularities on polyhedra in the finite element method. *SIAM Journal of Numerical Analysis* **33**, 729–759 (1996)

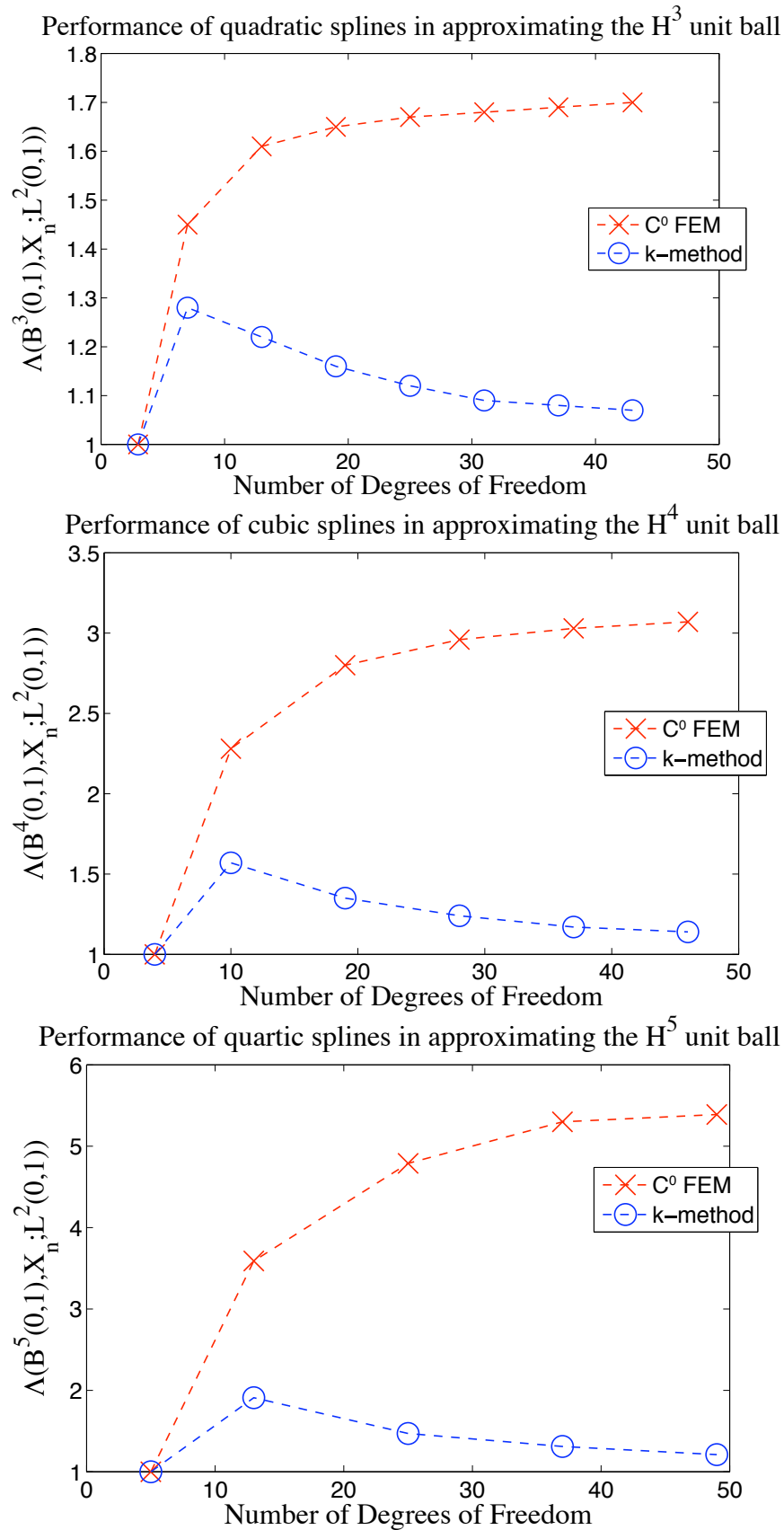


Figure 18: Performance of the classical finite element and  $k$ -methods:  $L^2$  optimality ratios

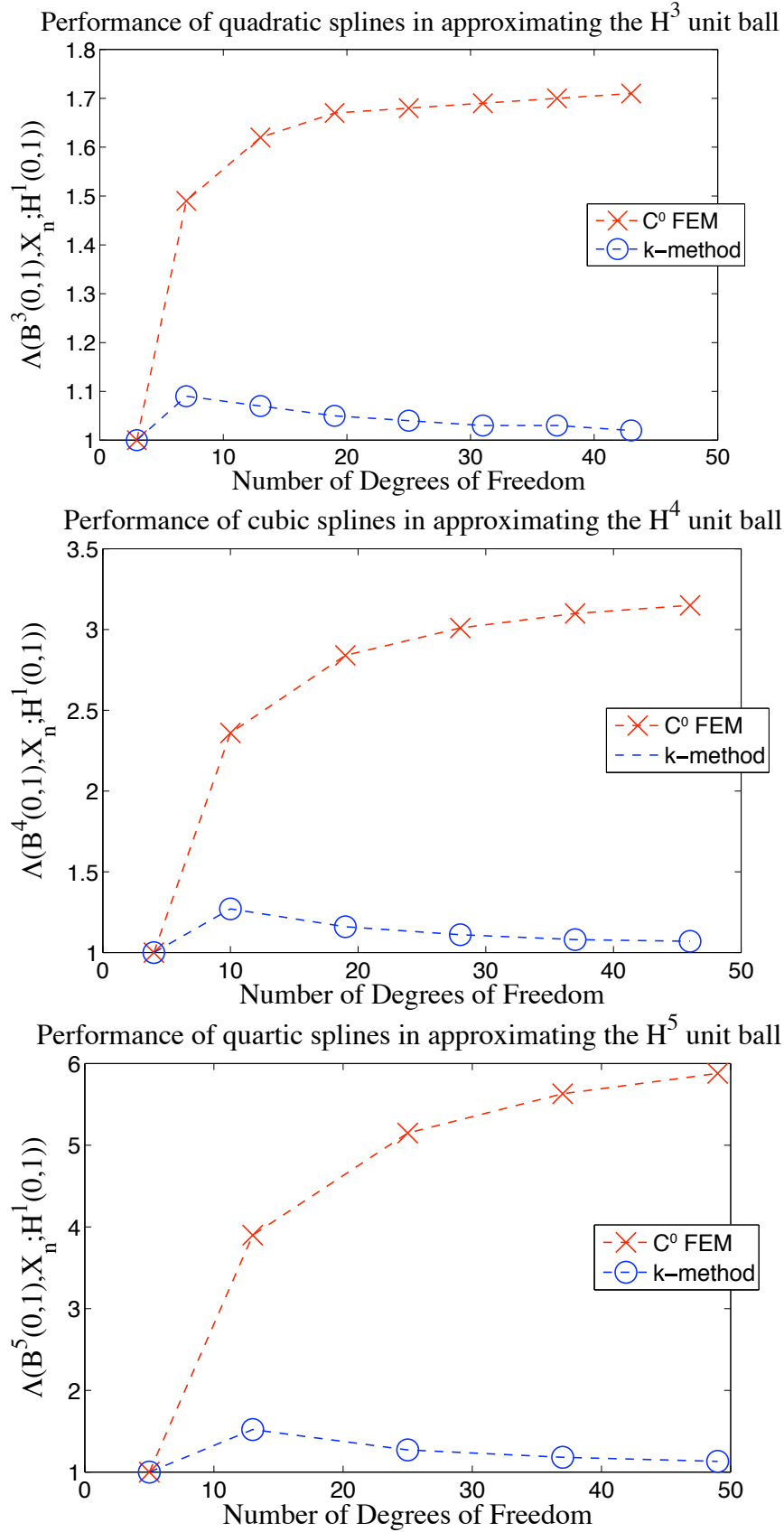


Figure 19: Performance of the classical finite element and  $k$ -methods:  $H^1$  optimality ratios

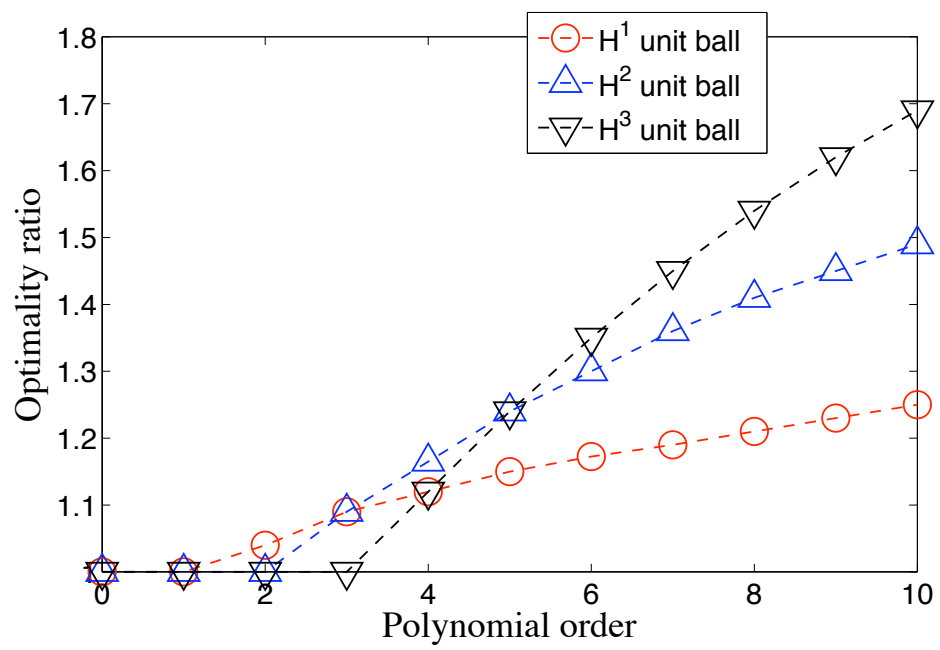


Figure 20: Performance of the spectral method:  $L^2$  optimality ratios